DESIGN AND SIMULATION OF A SOLAR THERMAL COOLING SYSTEM FOR NATIONAL MEDICAL STORES

BY

MARTIN MBAGA

(B.Eng. Mech. &Manuf. Eng., Kyu)

17/U/GMEM/17419/PE

A DISSERTATION SUBMITTED TO THE DIRECTORATE OF RESEARCH AND GRADUATE TRAINING IN PARTIAL FULFILLMENT OF THE REQUIREMENTS FOR THE AWARD OF THE DEGREE OF MASTER OF SCIENCE IN ADVANCED MANUFACTURING SYSTEMS ENGINEERING OF KYAMBOGO UNIVERSITY

OCTOBER 2024

DECLARATION

I Martin Mbaga, declare that the contents of this dissertation are my original work and have not been used in any other university for any academic award, or any other related reasons.

Signed; .... Date; 24/10/2024

APPROVAL

This is to approve that the work included in this dissertation was solely written by Mr. Martin Mbaga, a Master's student and was authentically carried out under my supervision.

Signed: .... Date: 7/11/2024...................................

Dr. Al-Mas Sendegeya

Signed: .... Date: 24/10/2024...................................

Dr. Samuel Kangwagye

DEDICATION

I dedicate this dissertation to my Dear mum Mrs. Margaret Mbaga, my brothers Allan, Aaron, David, and Rodney, my sisters Charity, Cossy, Diana, and Lillian, and my lecturers and friends who supported me and contributed to the achievement of this great step in my life.

ACKNOWLEDGMENT

Acknowledgment goes to my supervisors Dr. Al-Mas Sendegeya, and Dr. Samuel Kangwagye, Dr. Maureen Nalubowa Sempijja, the H.O.D Mechanical and Production Engineering, Dr. Catherine Wandera, Mr. Ongom Christopher and my colleagues and course mates for all the guidance, information, support and help given to me during this research.

TABLE OF CONTENTS

LIST OF FIGURES

LIST OF TABLES

ABSTRACT

Solar energy is a clean form of energy that is essential for nearly all natural processes. Solar thermal cooling offers multiple advantages compared to conventional electrically powered systems. A study was conducted to design and simulate a solar thermal cooling system for the cold storage facility at the National Medical Stores, to solve the problem of the high electricity cost incurred while running the current cold storage cooling system. The system was designed using assorted calculations and the respective parameters were acquired, it was modeled and simulated, to use flat plate collectors and a LiBr-water absorption chiller. The solar-powered absorption cooling system simulation was carried out using the TRNSYS simulation program, with weather parameters for Kampala, Uganda where the facility is located, and the results indicated that the system is viable and applicable, and can provide the required cooling sufficiently. To ensure continuous system performance and increase reliability, a 119m^3 hot water storage tank was included in the system, to ensure that the system can continue running for 48 hours for periods when there is no solar radiation. The system was designed with a capacity of 315kW (89.6 refrigeration tons), a 1,487m^2 flat plate solar collector tilted at 10^0 to the horizontal, and its coefficient of performance (C.O.P) determined as 0.667. The system was successfully designed and simulated and the development is recommended for National Medical Stores in order to control the high costs of electricity that are generated from using grid power.

Key Words: Trnsys, Absorption Chiller, Lithium Bromide, Solar, Thermal energy.

CHAPTER ONE: INTRODUCTION

1.1 Background

Globally, there is an increasing energy demand, arising from the continuously growing infrastructure leading to high energy requirements (Gevorkian, 2012). Different energy sources are utilized to satisfy the respective energy requirements and these include; fossil fuels for example, oil and natural gas, renewables like solar power, wind, hydroelectric power and biomass, nuclear energy, geothermal energy, hydrogen and biofuels (Dudin et al., 2019). According to (International Energy Agency et al., 2021), coal remained the dominant source of energy providing 37% of global energy requirements, renewable energies providing 27%, natural gases 24%, nuclear energy 10% and oil providing only 2%.

Over the years, various renewable energy solutions have been explored, and solar power has emerged as a reliable substitute to traditional energy sources, providing sustainable and reliable solutions for both industrial and domestic applications (Antonia et al., 2021). According to (Ministry of Energy and Mineral Development, 2019), there is still a need to explore and utilize renewable energy in Uganda to support the other existing power sources like hydroelectricity, bagasse, and oil. Solar power provides only about 5% of the total power used in the country and therefore, the government encourages more utilization of solar energy since it contributes greatly to the sustainable development goal number 7(ensuring access to clean and affordable energy) (International Energy Agency et al., 2021). Also, one of the greatest benefits of solar power is the Provision of energy with reduced greenhouse gas emissions and long-term cost savings.

The storage facility at National Medical Stores (NMS) has a section of 9 cold storages, used to store special vaccines and other assorted drugs at temperatures between 8^0C to -20^0C as recommended by (ASHRAE handbook, 2017). This is done before transferring the medicines to other smaller storage facilities in different upcountry locations for eventual administration. Each cold storage has two sets of cooling machines, which must run for 24 hours to achieve the required temperatures. According to (National Medical Stores, 2023), this cold storage facility consumes about 437.5kWh of power per hour, which sums to 10,500kWh per day hence generating a high cost of 4,848,900Shs per day at 461.8shs per kWh (unit). This research, therefore concentrated on designing and simulating a solar thermal cooling system to supply chilled air to the cold storage facility at National Medical Stores Kajjansi, to reduce energy costs accumulating from its respective day-to-day operations.

1.2 Problem Statement

The cold storage system at NMS is either run using the national grid or heavy duty standby generators whenever there is load shedding. The national grid provides unreliable supply of power due to consistent load shedding and this leads to intermittent use of standby generators increasing the cost of operation even more. The equipment have to run constantly for 24 hours, and since this system has to run for that long, the power consumption rate is 7,560kWh per day which yields about 3,491,208 Uganda shillings, contributes to very high operation costs. This therefore led to the need to design a reliable solar thermal cooling system, to act as an alternative solution to handle all the cold storage facility cooling requirements, at National Medical Stores warehouse in Kajjansi.

1.3 Research Objectives

1.3.1 Main Objective

The main objective of this research is to develop a solar thermal cooling system for the cold storage facility at National Medical Stores.

1.3.2 Specific Objectives

The specific objectives of the study were:

- **i.** To determine the cooling requirements of the cold storage system at National Medical Stores.
- **ii.** To determine the components and parameters of the solar thermal cooling system
- **iii.** To size the components of the solar thermal cooling system
- **iv.** To perform a simulation of the solar thermal cooling system

1.4 Research Questions

The questions that guided the investigations in the study are:

1. What are the cooling requirements of the cold storage facility at National Medical Stores?
2. What components make up the solar thermal cooling system?
3. What are the specifications of the solar thermal cooling system components?
4. What are the performance expectations of the designed solar thermal cooling system?

1.5 Significance

The main power source is grid power however during times when there is load shedding, heavy duty standby generators are used which consume a lot of fuel to run the facility as required, and equally generate a high cost of operation. This high power consumption resulting from the cold storage operation therefore leads to high operation costs. Developing and installing the solar thermal cooling system for the cold storage facility would thus reduce the costs arising from the operation of the cold storage facility and contribute to sustainable development goal seven (7) by ensuring access to affordable and clean energy.

1.6 Justification

National Medical Stores uses solar to power lights, computers, office equipment, conveyor systems, and charging of electric forklifts. The existing cold storage system however, is powered using the national grid, due to its high-power requirements for its daily operations. This is because the facility has to be run consistently at full capacity to enable the required temperatures for cooling the assorted medicines and vaccines all through the day and night. This high-power consumption from the cold storage system therefore leads to high costs being generated from a lot of power consumed in the operation process. The solar thermal cooling design therefore, focused on providing a feasible solution to the high-power costs by providing a renewable energy solution that will reliably serve the cold storage energy requirements.

1.7 Scope

This study will be conducted at the National Medical Stores warehouse in Kajjansi, where the cold storage facility is located, for six months. The study will involve determining the energy requirements of the cold storage facility, designing a solar power system that will satisfy the requirements, simulating the developed system to ensure reliable performance, and carrying out a cost analysis to ascertain the economic effect of the system when installed.

1.8 Conceptual Framework

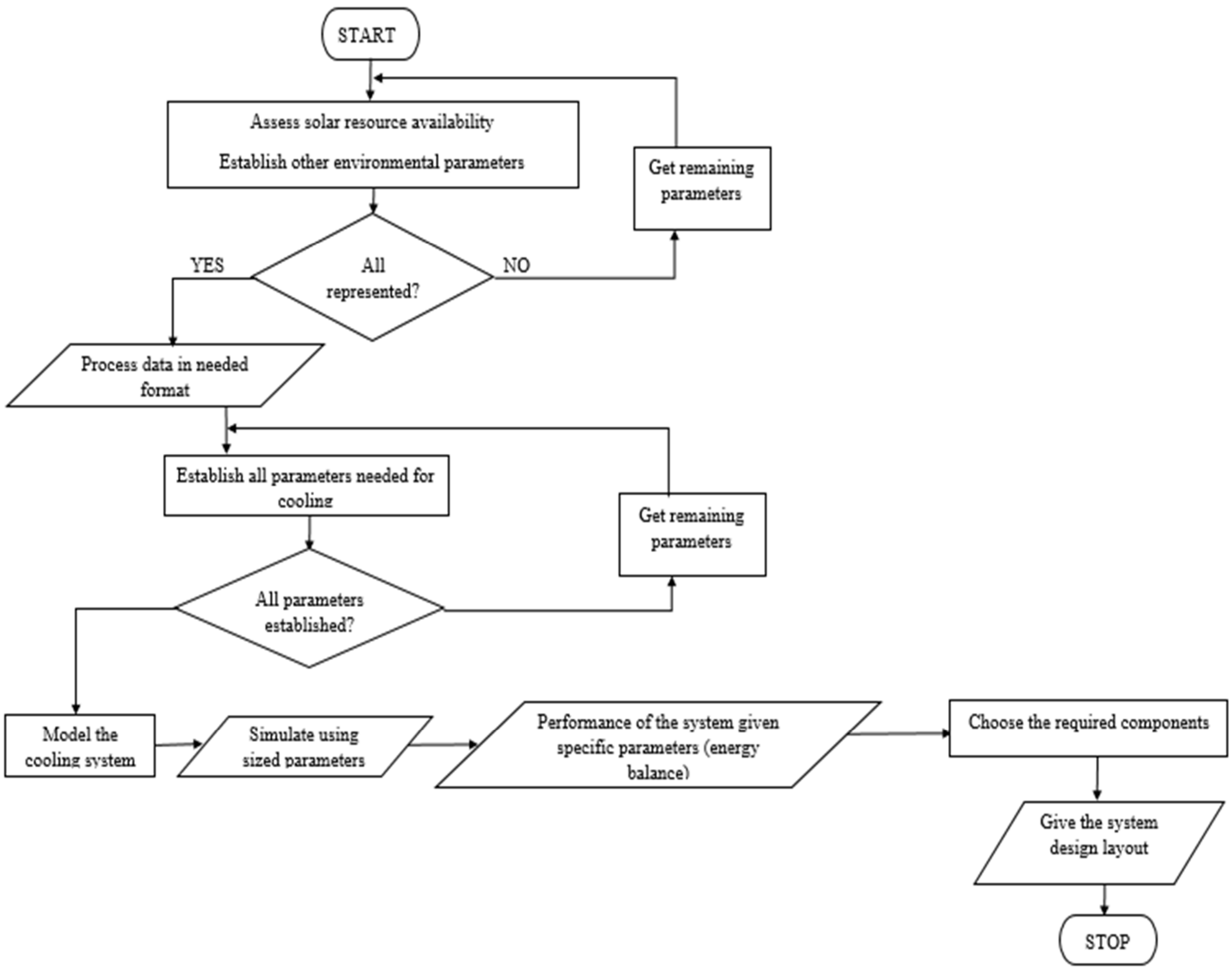

Figure 1.1: Conceptual Framework

CHAPTER TWO: LITERATURE REVIEW

2.1 Introduction

A summary of previously conducted research on cooling systems powered by solar energy, is presented in this segment. The sole reason for this analysis was to provide a thorough examination of the previous research and literature on solar driven cooling systems, with the ultimate goal of this study to identify areas where further research is necessary and to determine any gaps in knowledge.

2.2 Solar Energy

This type of energy is generated when the sun releases electromagnetic radiation through fusion reactions. This radiation reaches the Earth’s surface in form of electromagnetic rays, which can then be harvested and transformed into various resourceful types of energy (Delač et al., 2018).

The sun, continuously radiates energy at a rate of 3800×10^{20} kW. This energy is referred to as solar energy. Out of this massive amount, only about 1800×10^{11} kW is received by the Earth's surface. However, not all this emitted energy descends to the Earth's surface. About 50% is absorbed by the Earth's atmosphere and clouds, and only 40% reaches the surface. The rest gets redirected back to space by the Earth's surface, clouds, and atmosphere (Hang et al., 2013). Studies have shown that converting just 0.1% of the energy that reaches the Earth's surface into usable energy would satisfy the global total energy generating capacity of about 3×10^3 GW and beyond. If we could increase the efficiency of this conversion to 10%, we could generate even more energy, all from a virtually unlimited source of clean energy. Solar energy has the ability to transform the energy systems of the world. The technical potential of solar energy is much greater than the global electricity requirement; it is a clean, renewable, and abundant source of energy that can power everything from homes to industries, and even entire cities. (Gupta, 2014)

Over time, various technologies have been developed to harvest solar energy for various domestic and industrial functions.

2.3 Solar Photovoltaic as Compared to Solar Thermal

Comparing the two forms of solar energy, solar thermal is more efficient than solar photovoltaic, since they capture and exploit more amounts of solar radiation. In photovoltaic units, a significant amount of collected radiation is lost as heat, which cannot be converted into electricity (Montagnino, 2017). However, thermal energy harvesters are designed to directly convert the collected energy into heat without any such limitation, and as a result, a very high efficiency (up to 95%) of a solar thermal collector can be obtained.

2.4 Basics of Cooling

According to Delahunt (2016), cooling is the process of providing and maintaining a desired temperature to a specified enclosed area and this temperature should be below that of the surroundings. Cooling technology has a variety of important applications, such as in air conditioning systems for human comfort and for preserving fragile goods by providing respective required temperatures for their storage. Space cooling involves controlling air cleanliness, temperature, moisture content, scent, and air circulation, to offer comfort to the occupants, achieve a desired process, or provide required storage for a product. Cooling can be attained through various ways; the refrigeration cycle and vapor absorption, among others.

2.5 Solar Cooling

Systems which are solar-driven are advantageous for using more environmentally friendly operating fluids such as water or salt solutions. In addition to being energy-efficient, they are ecologically friendly. They can serve as detached systems, or in conjunction with standard air conditioning units, to improve air quality for different respective buildings. The main aim of SCS is to provide more energy-sustainable solutions while reducing CO_2 emissions using zero-emission technologies.

Conventional cooling systems release environmentally harmful gases into the atmosphere, contributing to greenhouse and ozone depletion effects. Developing solar-driven cooling technologies has become a key global research area, with the potential to mitigate global warming by contributing through solar-assisted refrigeration and cooling technologies. Amongst other technologies, absorption chiller cooling has a promising global market potential (Tsoutsos et al., 2010).

Solar energy has become an increasingly popular solution for cooling systems, especially in situations where electric energy is scarce or expensive. Research by (Boopathi Raja & Shanmugam, 2012) suggests the method that uses single-effect absorption cooling using LiBr–water as the working fluid is recommended for domestic purposes, and flat plate and evacuated tube solar collectors to be more reliable and feasible for this specific system.

Two important parameters need to be considered in order to define the most cost-effective solar cooling system;

1. The cost of acquiring the solar energy collectors and storage equipment.
2. The deliverable performance of the system.

Based on these parameters, the following suggestions are given to provide an efficient system;

(i) The system should be designed to follow the thermosiphon principle, where the tank is placed at a location above the collector, and heat is transferred after the collection by the transfer fluid to the hot water storage tank.

(ii) The movement of hot water from the tank to the generator can be controlled by installing the later inside the stratified storage tank, minimizing the cost of insulation.

(iii) The solar-powered absorption system has a significant advantage over a compression system when it comes to operational costs. This is mainly because it utilizes three main electrical equipment: - a pump, a condenser fan, and a cooling coil fan. Although the primary cost may be high, there are various options to reduce the system's cost of operational in the long run. Ultimately, this means a single effect solar-powered absorption chiller can be as competitive as a compression system with regard to long-term operation.

Generally, while the initial cost of a solar-powered single-effect cooling system may be higher than the compression system, there are various options for reducing operational costs over time, making it an attractive option for those looking for a more sustainable and cost-effective cooling solution (Prasartkaew & Kumar, 2010).

2.6 The Solar Thermal Cooling System

A solar cooling system utilizes solar energy to yield ice-cold water or air for air conditioning purposes. The system works by using solar collectors, which are modules equipped with heat-absorbing materials that are designed to capture sun rays. As the sunrays strike these collectors, the modules' material absorbs the solar radiation, getting heated up in the process. The heat is then passed on to a fluid that circulates within the collectors through tubes and is used to drive the operation of an absorption chiller. The absorption chiller utilizes the heat it is supplied with, to supply the energy needed for the absorption refrigerant cycle to deliver chilled water or air. Chilled water or air is produced by the system and is distributed throughout a building or air space to provide the desired cooling effect (Montagnino, 2017).

Solar cooling technologies are environmentally friendly and contribute significantly to reducing carbon emissions that cause the greenhouse effect. The most frequently used technology for solar cooling is the thermal-driven lithium bromide chiller. The single-effect type of Lithium Bromide -water absorption chiller has the benefit of powering by the normal collectors; either flat-plate or evacuated tube which are easily accessed on the market, and this is due to their able operating temperature range to drive thermal energy (Zhai et al., 2011). Solar cooling systems that are currently available are primarily based on single-effect chillers that use Lithium Bromide-water ($LiBr$-H_2O). These absorption chillers are a proven technology and are available in both evacuated tube and flat-plate collectors. According to research about solar-powered single-effect absorption cooling systems, the LiBr–H_2O absorption chillers are most preferred for solar applications, because, solar collectors can power the generator of the absorption system cheaply (Florides et al., 2003).

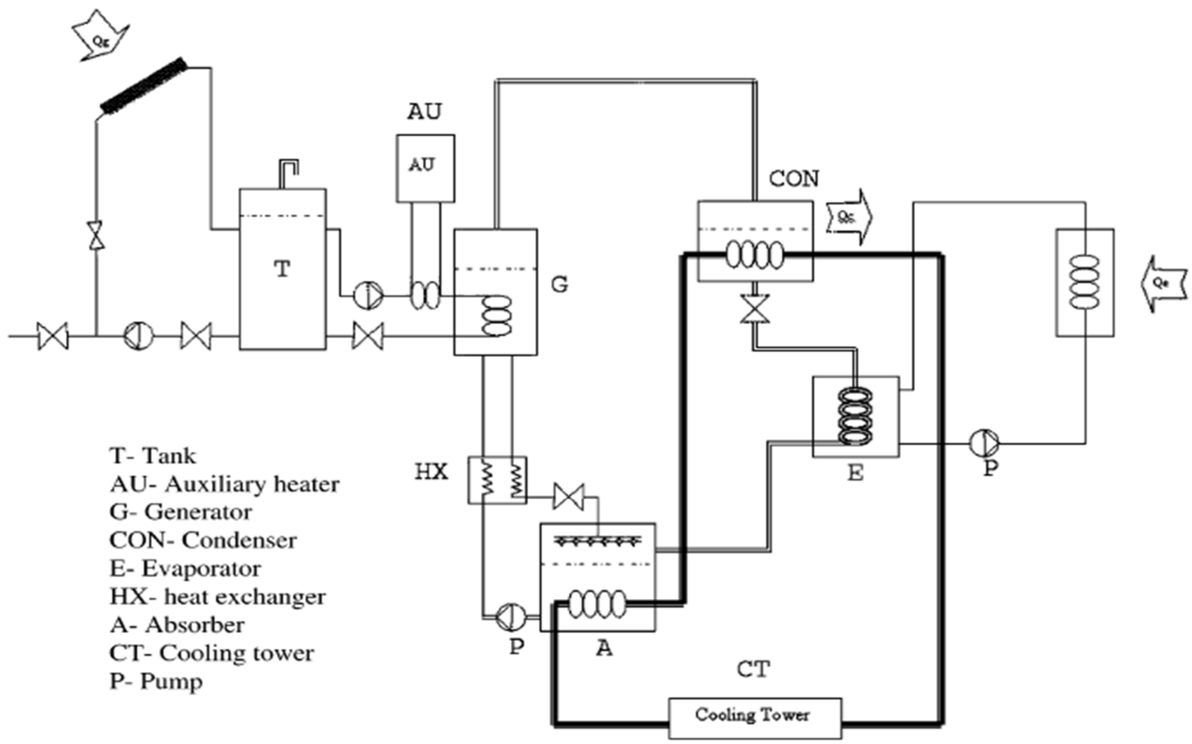

Figure 2.1: Standard solar powered air conditioning system layout (Perez-Lombard et al., 2011)

2.6.1 Cooling Procedure

During cooling, the absorption chiller is fired up by the heat from the heat storage to produce the required cooling. The flat plate collectors, collect thermal energy from the sun's radiation, and use it to increase the temperature of the fluid (water) used to transfer the heat. After absorbing the heat, the hot fluid is then stored in a thermal tank for later application. Whenever there’s need, the hot water is transferred to the LiBr-Water absorption chiller where it dissipates its heat to the generator of the absorption chiller. After this dissipation, the hot water is now cooled and returned to the storage tank to continue the process. The effect of cooling is experienced in the evaporator, where the water is cooled and sent to the fan coil. The fan coil uses the cooled water to cool the air that is supplied to the target space to be cooled. The cooling tower provides continuously flowing water which extracts heat from the condenser and absorber parts, keeping the system properly cooled.

Solar air-cooling systems are an eco-friendly and energy-efficient solution for cooling purposes. These systems have a lot of advantages as they rely on solar energy, which leads to reduced energy consumption, environmental benefits, and potential cost savings. Solar-driven air cooling systems are a great way to conserve energy and promote sustainable cooling methods. They also provide an opportunity to achieve energy independence in areas where electricity access is limited (Rasuli & Torii, 2023). However, some challenges prevent a wider adoption of these solar energy systems and these include; the high costs involved in installing such systems, lower efficiency compared to traditional energy sources, the need for effective energy storage solutions, the available space for solar panel installation, the impact of climate variations, the complexity of integrating these systems with existing HVAC infrastructure, and a lack of public awareness.

Solar air conditioning systems are a promising solution for cleaner and sustainable cooling. Although challenges exist, ongoing research and development efforts are addressing these issues, driving innovation and paving the way for the widespread adoption of solar air conditioning systems (Mahmood Aljamali et al., n.d.) and (Rasuli &

Torii, 2023). Cooled air production using absorption cycles is a popular use of solar thermal power, with absorption systems standing out as the most advanced solar cooling technology. To determine the most economically efficient solar cooling system, key factors like the investment cost of the complete system, the refrigerant's performance coefficient, and the accessibility of solar energy resources are considered. In short, solar air cooling stands at the forefront of the energy transition, offering a promising path toward a greener future.

2.6.2 Components of the Solar Thermal Cooling System

These comprise different components, which serve different purposes that each contributes to the whole system’s main function. The major solar thermal cooling system components are explained below:

2.6.2.1 Solar Collectors

These are special modules or panels mounted on the roof of the building or in an area where they are sufficiently exposed to sunlight. All typical solar thermal collectors are made up of a glazing exterior, an absorber material, header tubes, insulation, and a case. The heat-absorbent material absorbs radiation from the sun, and transforms it into heat that can directly be used or stored in hot water tanks. The collected heat energy is thereafter transported by a heat transmission fluid which is any of the fluids like air, water, or any other special fluid (Mahmood Aljamali et al., n.d.). Low-temperature solar collector markets are well-established and there are various solutions available that are technically advanced. These include flat-plate panels that operate between 70-80°C and evacuated tube collectors that are capable of reaching temperatures over 100°C. The safety and efficiency of these systems have been improved over time through the introduction of concepts such as drain-back systems and offline recirculation. These collectors are commonly used in SHC systems alongside single-stage absorption cycles (Henderson et al., 2005).

The main types of solar collectors are stationary collectors and concentrating collectors. Stationary collectors, also known as non-concentrating collectors, intercept solar radiation in the same area where it is collected. The device is typically fixed and does not move, and the radiations are absorbed and immediately transformed into energy in the same area. These specific collectors are commonly used for domestic and commercial solutions, such as heating water or providing electricity. In contrast, a concentrating solar collector intercepts solar radiation over a bigger area compared to the area of collection. The radiation is then concentrated to a smaller area where it is collected and converted into the required energy. This type of collector is mostly used for power generation on large-scale, such as solar thermal power plants.

The ratio of interception area to collection area is referred to as the concentration ratio. A greater concentration ratio means that more solar radiation is being collected and converted into energy, which can result in greater efficiency and output.

A. Stationary Solar Collectors

The types of stationary collectors are;

i. Flat Plate Solar Collectors (FPC)

These are elaborated as in the figures 3 and 4. The collectors work by allowing solar radiation to pass through a transparent glazing and onto an absorber plate. The plate absorbs a large solar energy amount from the radiation, which is then transferred to a fluid in tubes. This energy in the fluid can be either used directly or stored for later use. To reduce heat losses, the absorber material and case sides are insulated. The glazing is also important because it minimizes convection losses and radiation losses since the glass material limits long-wave thermal radiation from passing through, and this creates a greenhouse effect and contributes to the collector's efficiency (Mahesh, 2017).

Flat plate collectors are entirely stationary and don't require sun tracking. They are always installed slanted towards the equator, which is the major reason why they are always installed facing north and south in the southern and northern hemispheres respectively. For the collector, the slope should always be kept equal to the local latitude adding 10^o.

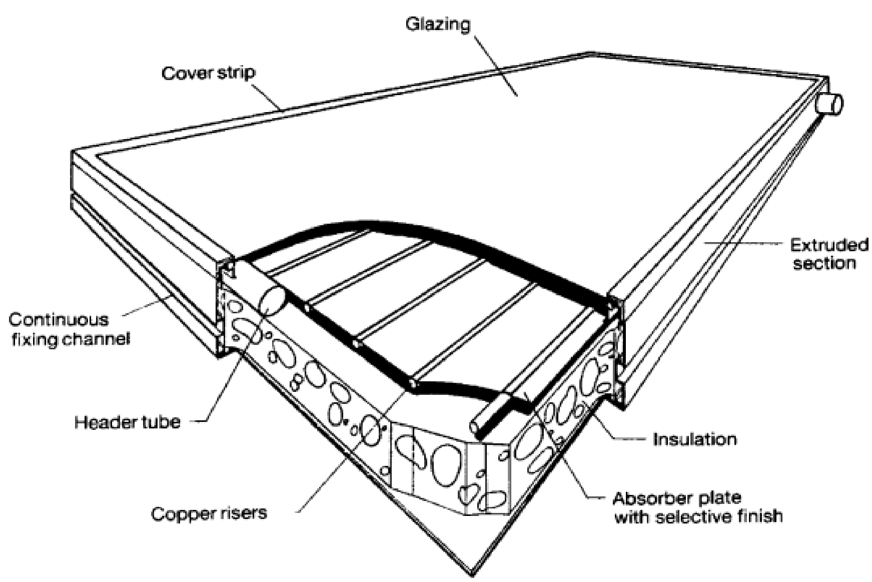

Figure 2.2: Assembled Flat Plate Collector (Mahesh, 2017)

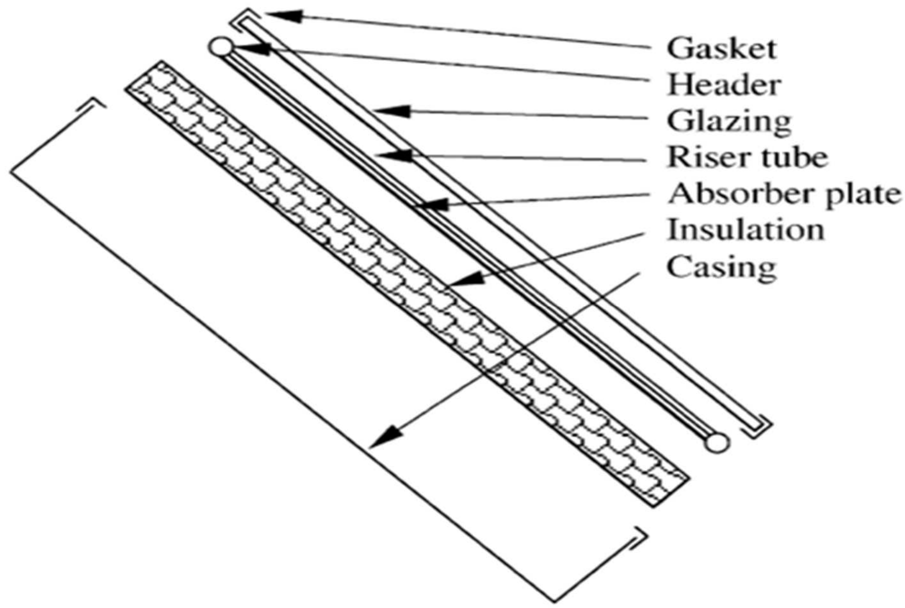

Figure 2.3: Disassembled flat plate collector view (Mahesh, 2017)

The major components of the Flat Plate Collectors are;

1. Glazing: A glass layer or any material that transmits radiation.
2. Absorber plates: Flat plates, ridged surface where tubes are attached, in which the heat transfer fluid flows.
3. Headers: These enable the admission and discharge of the respective heat transfer fluid into the collector assembly.
4. Insulation: This minimizes the thermal losses from the collector's bottom side to the surroundings.
5. Casing: Surrounds the system modules keeping them dust free, controls the humidity content, and limits other external substances that might interfere with the systems' operation. The FPCs are widely preferred because they are able to collect thermal energy cheaply.

ii. Stationary Compound Parabolic Solar Collectors (SCPC)

SCPCs are designed to mirror the incoming radiation received within the area of collection, to an absorber. Here, double sections of parabolic-shaped collectors are joined facing themselves, to enable solar radiation reception from either side without tracking the sun as shown in Fig. 5. It uses numerous internal reflections where, the radiation that gets in contact with the space within the collector reception angle, is directed to the absorber at the lowest point of the collector (Alazazmeh & Mokheimer, 2015). In the SCPC, the sections (BA and CA) of the reflector should be kept circular, while the upper sections (DB and EC) should be kept parabolic. The absorber tube to which the heat is concentrated, gathered, and transferred to a thermal transfer fluid is represented by T.

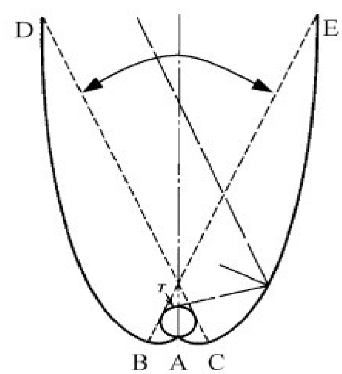

Figure 2.4: Compound parabolic collector (Gupta, 2014)

iii. Evacuated Tube Solar Collectors (EPC)

This type of collector consists of a high-temperature pipe, placed within a vacuum tube. This design allows the vacuum cover to reduce losses that may occur due to conduction and convection, resulting in higher temperatures being achieved compared to the flat plate collectors. These can absorb direct and diffuse radiations, and have a greater efficiency at lower incidence angles, leading to improved performance throughout the day. The materials used for heat transfer are vaporized while absorbing heat. Each of the high-temperature pipes contains a little fluid, which evaporates and condenses, such as methanol. The collected thermal energy causes the liquid to evaporate, once it reaches the heat sink region, it condenses releasing its latent heat for further application. The condensate is then returned to the collector, to continue the process cycle (Mahesh, 2017). The EPCs are generally designed to suit locations with high levels of solar radiation. The benefits of Evacuated tube solar collectors are highly compromised during periods when the weather is not friendly; like on cold, rainy, and windy days.

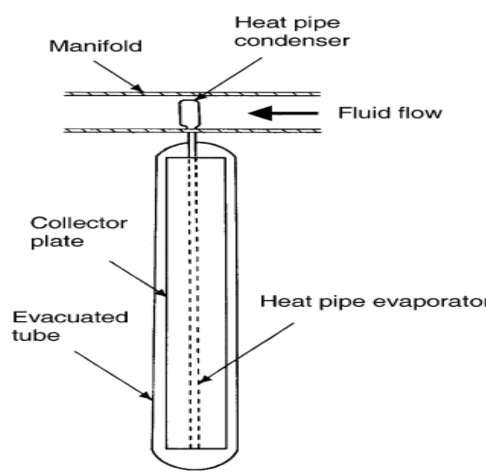

Figure 2.5: Evacuated Tube Solar Collector (Mahesh, 2017)

B. Sun Tracking Concentrating Solar Collector

To achieve high heat transmission fluid temperatures, it is necessary to collect solar radiation on a small area. Concentrating collectors are used to focus solar rays onto a specific point or surface, which is then transformed into heat energy. This is achieved using mirrors or lenses to reflect or refract the radiation. The reflected or refracted radiations are then all directed towards a focal point, and therefore this increases the intensity of energy at the receiving surface and thus increases the fluid temperature.

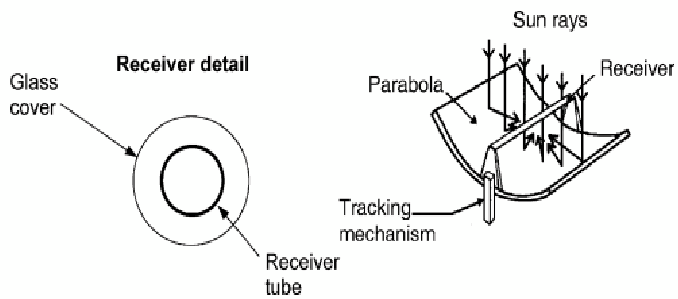

Parabolic concentrating collector

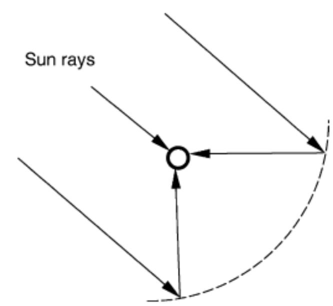

Fresnel type Polar Tracking Collector

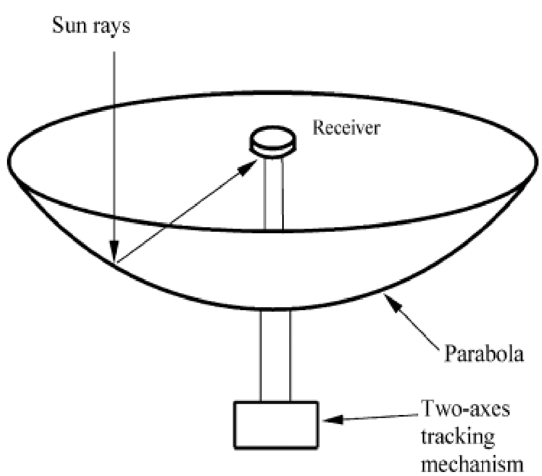

Concentrating dish collector

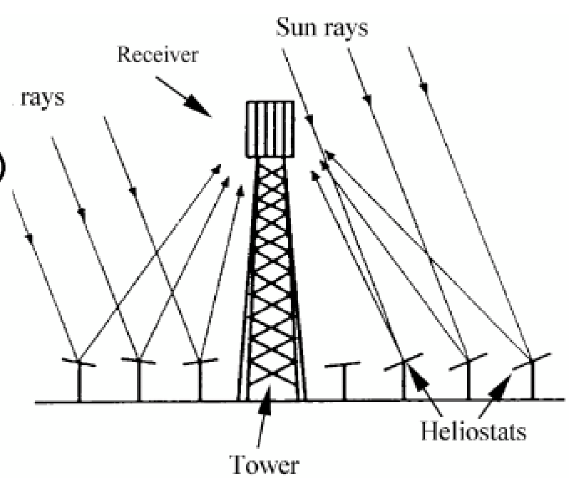

Concentrating Tower system

Figure 2.6: Concentrating collectors (Gupta, 2014)

2.6.2.2 Heat Transfer Fluid

The heat transfer medium, often water, circulates the solar collectors using tubes. While it passes through the collectors, it absorbs the heat that was initially collected from the solar radiation and proceeds with its circulation to the next stage in the system.

The collectors are well designed to absorb sun rays and convert them into thermal energy and at this stage, the heat transfer medium circulates the heat, through a series of tubes that run through the solar collectors. This heat is then carried by the fluid as it continues its circulation through the system either for immediate utilization or stored for future use (Monné et al., 2011). The process of heat transfer efficiency, is critical for the effectiveness of the solar system since any loss of heat or inefficiency in the transfer process would significantly reduce the general system operation. Therefore, it is critical to use high-quality materials, ensuring the system is correctly designed and installed to maximize heat transfer efficiency.

2.6.2.3 Thermal Storage

Thermal storage is mainly a stratified tank that is used to store excess heat harvested, to be used mainly during periods when there is no sunlight, for example at night or on rainy and cloudy days. Thermal storage also contains a heat exchange provision which allows heat transfer from the heat transfer liquid to another fluid that's used in the absorption cycle. The fluid that is mostly used in the concentration cycle is a lithium bromide-water solution or a suitable absorbent refrigerant according to the respective system design.

A properly insulated thermal tank controls different heat losses and can retain thermal energy for several days, incorporating one into a solar thermal cooling system, therefore, would improve the system's efficiency (Sumathy et al., 2002).

One of the highly recommended storage tanks is the stratified thermal storage tank (Ganguly, 2016). This specific type of thermal storage facility is preferred in solar thermal systems because it is characterized by a special capability to maintain temperature differences at the respective water levels in the storage facility. There is a limitation to any mixture of the water in the layered storage tank hence a significant temperature difference between the upper water (hotter) and the one at the lower (less hot) end of the tank.

While small thermal storage tanks smoothen the variations, larger storage units can be loaded by solar radiation to make the thermal energy available for many more hours after sunset or early morning for pre-cooling purposes. Respective Storages can be designed to accumulate heat either from the solar field or the cooling generated by the chiller if a close cycle unit is adopted (Montagnino, 2017).

2.6.2.4 Absorption Chiller

The actual cooling procedure happens in the absorption chiller, which is an alternate process for the conventional refrigeration system; the vapor compression system. The cooling effect in the absorption chiller is produced by inputting thermal energy which becomes the driving parameter for the process. Absorption chillers usually have their operation driven by one of the liquid solutions, either Lithium Bromide-water ($LiBr-H_20$) or ammonia-water (NH_3-H_20), which operate as refrigerant and sorbent, respectively (Zhai et al., 2011). Considering standard operations, single-effect absorption chillers can be driven between 80–100^{0}C, a compatible range with the temperature provided by static solar collectors.

Single effect Lithium Bromide–water absorption chillers are widely analyzed based on performance, and according to the general agreement, they present an established option with a good solution for a deep breakthrough into the building market (Ali et al., 2008).

This system is comprised of four (4) units; the condenser, thermodynamic generator, evaporator, and absorber. It uses the absorption refrigeration cycle principle to achieve the cooling required. In the absorption chiller, a refrigerant (water) is absorbed into a liquid absorbent (LiBr) in the absorber. Heat is applied to the absorber from an external heat source, vaporizing the water from the LiBr. The vapor refrigerant is then sent to the condenser, and it releases heat and is condensed to liquid. The liquid refrigerant returns to the absorber, and the cycle repeats.

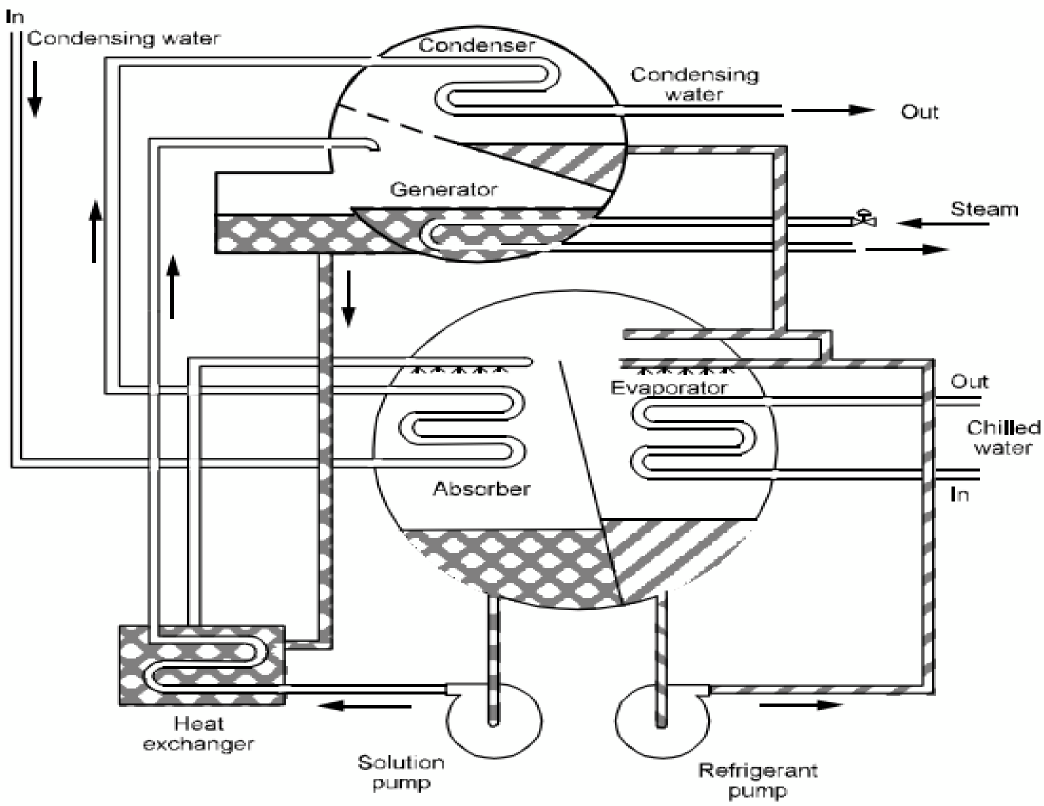

Figure 2.7: Schematic of absorption chiller ***(Eicker & Pietruschka, 2009)***

The absorption procedure occurs in two sections, the upper one which contains the condenser and generator, then the lower one which comprises the evaporator and the absorber units. The thermal input at the generator, causes the water in the LiBr-water solution to evaporate. The evaporated water then goes through the condenser and is condensed by a cooling medium into a liquid. The liquid proceeds to the evaporator, absorbing heat from the cooling fluid, and creating the desired cooling effect. The absorber-evaporator section operates at very low pressure, hence decreasing the boiling point, thus water boils and evaporates at a very low temperature (Delahunt, 2016) & (Florides et al., 2003). The water vapor is then carried through the absorber, gets absorbed into the highly concentrated Lithium Bromide solution, is absorbed by the solution, and creates a weak solution which is pumped to the generator, and the cycle is repeated to generate a cooling result at the evaporator.

The LiBr-H_2O absorption chiller contains independent external fluid loops for its complete operation;

1. The input loop of heat into the generator
2. The water loop to the cooling tower
3. The Cooled water loop for delivering the required cooling effect.

2.6.2.5 Cooling Tower

This is an essential component of large cooling systems that use absorption chillers. It helps to control the circulating temperature of the water in the chiller system. Cooling towers have a water storage tank that stores cold water for the cooling process, this water is circulated in the system through pipes and absorbs heat from the absorption chiller unit, after which, the water is then sent back to the cooling tower, and undergoes a process called evaporative heat rejection, which helps cool the water and release the absorbed heat into the environment. The cooled water is then recirculated into the chiller system to complete the cooling process (Zhai et al., 2011). Cooling towers are also called evaporative heat rejection devices and are essential for maintaining the efficiency and effectiveness of large cooling systems.

2.6.2.6 Fan Coil Unit

This is an equally crucial part of cooling systems which is used in diverse settings, including commercial, residential, and industrial buildings or applications. It comprises a cooling coil and a fan, and functions by exchanging heat from air to water and vice versa.

The cooling coil, which is responsible for removing heat from the air, is typically made of copper tubes and aluminum fins (Assilzadeh et al., 2005). The unit has a fan which is responsible for circulating the cooled air through the cooling coil.

The fan coil unit uses cold water as a medium to cool the air passing through it and transfers the heat it obtains, to the chilled water, which is circulated back to the chiller for cooling. Fan coil units have the advantage of using lower-grade chilled water to provide cooling to a specific space, making them highly efficient.

In summary, fan coil units are an effective and reliable way of providing cooling in various settings, and they offer flexibility in terms of their ability to utilize lower-grade chilled water.

Figure 2.8: Fan coil unit (Xu & Wang, 2017)

2.6.2.7 Control Systems

All modern cooling systems are equipped with a range of advanced components which include; sensors, controllers, and actuators that are responsible for optimal performance and energy efficiency (Ali et al., 2008). Sensors are responsible for constantly monitoring various system factors like temperature, pressure, and flow rates, while controllers receive this information and use it to make decisions about how to regulate the system. Actuators then work to adjust the system based on these decisions, ensuring that it continues to operate at an optimal level.

This constant monitoring and regulation of key parameters has several benefits. First, it ensures that the system operates safely and reliably, without any unexpected fluctuations that could cause damage or safety hazards. It also helps to improve energy efficiency by reducing any unnecessary energy consumption, which is achieved by ensuring that the system only uses the energy it needs to operate, rather than wasting energy on unnecessary processes.

Generally, the integration of these components into any of the systems is critical for the efficient and effective operation of the systems. By constantly monitoring and regulating key parameters, they help to ensure that the system operates smoothly and reliably, while also delivering efficient output while minimizing energy consumption.

2.7 Solar Thermal Cooling System Modeling

STCS modeling and simulation is an analysis process that involves the use of mathematical calculations and computer applications to analyze designed and operation cooling system performance. The process starts by developing a mathematical model that presents the physical items of the solar thermal cooling system, including items like solar collectors, heat exchangers, pumps, and cooling towers. The computer model results are then used to simulate the system's operation over time, considering different conditions, and inputs (Agyenim et al., 2010). The simulation can be used to evaluate the system's performance, identify areas of inefficiency, and optimize the system's design and operation. The simulation results give an operation prediction about the system's energy consumption, thermal efficiency, and environmental impact.

The simulation can also be used to evaluate different design options, like alternative solar collector types, heat exchangers, and cooling towers. By simulating the system's performance under different configurations, the designers can identify the most optimal design that will meet the system's performance requirements while minimizing the cost and environmental impact and settle for the optimal choice design. This process is crucial for implementation of the design for all efficient, reliable and economical solar thermal cooling system.

2.7.1 Transient System Simulation Platform (TRNSYS)

TRNSYS is a simulation program, used to analyze transient systems, especially designs for thermal systems. It is a model created by the Solar Energy Laboratory members at University of Wisconsin in 1998. Written in ANSII standard Fortran-77, it comprises several small routines that model respective system components. Each small sub-system has a mathematical model that is input according to terms of their ordinary and basic parameters, making it an ideal tool for simulating complex systems. With TRNSYS, users can easily identify all modules that constitute a respective system and formulate a comprehensive mathematical formulation for each (Florides et al., 2003). The respective type for each TRNSYS smaller routine used to model each component is presented in Fig. 10.

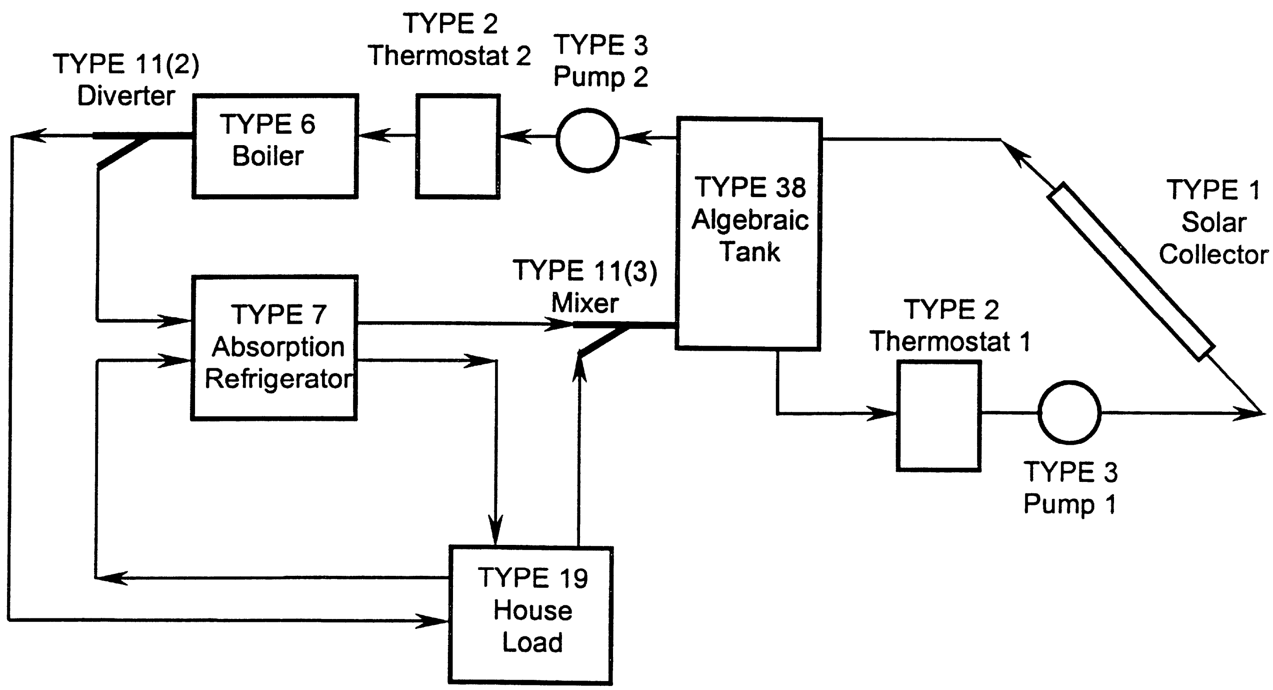

Figure 2.9: TRNSYS formats for creating a solar thermal cooling system modelling (Said et al., 2012)

The TRNSYS program models and simulates solar collectors, thermal storages, absorption chiller systems, and the cooling load delivered based on the climatic data of the site. The process of modeling and simulation is illustrated in Figure 11. First, the weather details at the site in question are determined, the specific components set up in the deck file, the specifications, data inputs and variables are defined, and then the program is executed. The model program produces charts and diagrams that are used to analyze the results, and thereby the most suitable components can be chosen (Said et al., 2012).

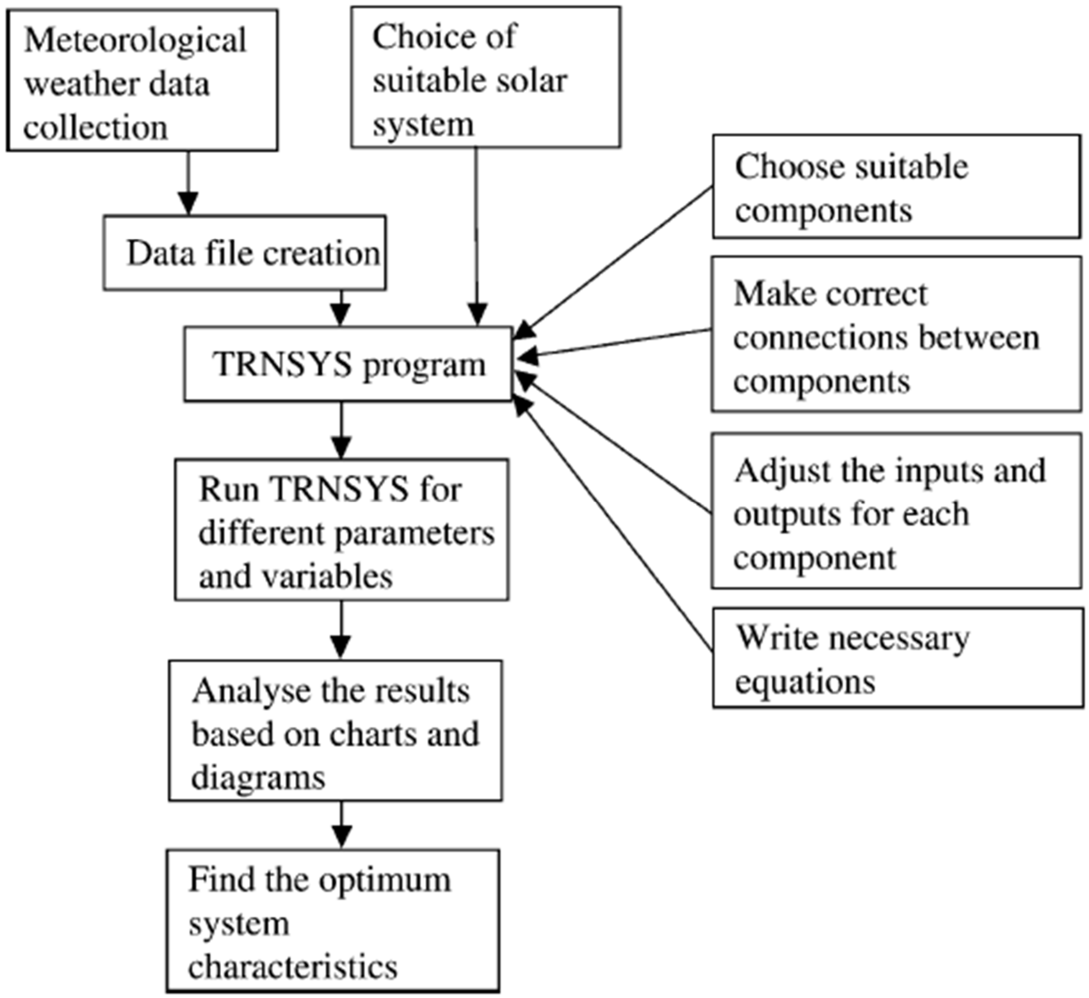

Figure 2.10: Solar thermal air conditioning model Flow chart (Assilzadeh et al., 2005)

Several assumptions are considered while simulating the designed system, according to observed and experimental findings from previous reports and published information on solar cooling research. These are important for creating a system that combines all components for an integrated simulation (Xu & Wang, 2017). These are;

(a) The fraction of solar represents the quantity of the generator load supplied by the thermal system, excluding consumption of power by other components such as pumps and controls.

(b) As the outdoor temperature is higher, the hot water tank is kept outside to minimize energy losses.

(c) There is no need to use heat exchanger and antifreeze solution amongst the collector water loop and the storage tank.

(d) The pump that circulates water in the collector loop turns on when the water outlet temperature from the collector and the temperature of the top layer of the storage differ by more than 3^0C, and stops when it becomes less than 0.5^0C.

2.7.2 Weather Specifications

For certain solar energy applications, it is important to have precise climatic data. The accuracy of the ambient temperature and solar radiation is particularly vital in these scenarios. This work requires the use of annual climate data for the relevant site, and it is important to consider variations in total radiation on the surface of the collector, normal direct solar radiation together with the global horizontal solar radiation (Assilzadeh et al., 2005).

2.8 Summary of key findings from the literature review.

Table 2.1: Key literature

S/No	Authors	System/parameters discussed	Results
1	(Montagnino, 2017)	Presented an evaluation about different types of solar systems including new developing technologies.	Discovered that single effect solar thermal systems are a preferred option for affordable and feasible solutions for mainly commercial large-scale operations.
2	(Zhai et al., 2011)	Presented new options of design regarding LiBr-H_2O solar absorption cooling systems mainly focusing on solar collectors, secondary systems, and cooling modes.	1. Double-effect absorption chillers were found more appropriate for air-cooled units in hot and dry regions. 2. Solar thermal energy harvesting and absorption unit performance are key aspects of the entire system cost. 3. When incorporated into the system, cooling towers can be eliminated. 4. The storage tank capacity was confirmed to be within the specific volume range of 0.01–0.08m^3/m^2.
3	(Qu et al., 2010)	A 16kW double-stage LiBr-water absorption solar thermal cooling system was developed and modeled in TRNSYS, using 52m^2 of parabolic trough solar collectors.	The solar collector performance was significantly impacted by their orientation, and the thermal storage ought to be located in the heat collection loop
4	(Marcos et al., 2011)	An air cooled experimental 4.5kW LiBr-H_2O solar absorption cooling and heating facility was developed, and it included a 1500liter thermal storage tank	1. During the period in question, the heating demand was met up to 65.3%, while the air conditioning demand was met up to 46%. 2. It took nearly 10m^2 of collectors to generate 1 kW of thermal energy for cooling. 3. For the absorption chiller, the average COP was 0.55.

		and a total collector of $42m^2$.	
5	(Palacín et al., 2011)	A 4.5kW capacity single-effect Lithium Bromide–water chiller was modelled using TRNSYS, examining two heat rejection mechanisms: a geothermal sink and a dry cooling tower.	1. When a dry cooling tower system is used, the COP is significantly affected by the temperature of the surroundings. 2. The system performance was improved by the geothermal sink, and this improvement was not affected by outdoor conditions.
6	(Monné et al., 2011)	TRNSYS was used to model a 4.5kW rotary absorption chiller with a LiBr-water solution and a dry cooler tower.	The COP was compromised by the temperature of the cooling water, but it could be improved up to 42% by utilizing a geothermal sink.
7	(Florides et al., 2003)	Discussed an 11kW simulation for a LiBr-Water solar thermal cooling system.	Successfully simulated the system with the optimized system, $15m^2$ with a recommendation for parabolic collectors and a 600litres hot water tank.
8	(Assilzadeh et al., 2005)	Created a solar LiBr-water absorption system design and TRNSYS simulation for Malaysia weather.	Optimized 1ton absorption chiller system with $35m^2$ of tilted collector at 20°, and thermal storage of size $0.8m^3$.
9	(Desideri et al., 2009a)	Presented two solar cooling case studies for industries and hotels.	Customized LiBr-H_2O absorption chiller using concentrating collectors with thermal storage are recommended for industries, and then a hybrid tri-generation system was recommended for hotels since it would produce electricity, heating, and cooling all in one.
10	(Eicker & Pietruschka, 2009)	Developed a complete model and simulated solar thermal LiBr-H_2O cooling systems, which were integrated with a	It was noted that: 1. A mass flow increase would lead to a reduction in the collector surface area and a further reduction in the system costs.

		layered storage tank and simulated using TRNSYS.	2. For a 3m^2 kW^{-1} solar collector, at 85°C and working with truncated flow circumstances, an 80% solar portion was achieved. 3. It is essential to carry out Dynamic simulations to achieve correct solar thermal system sizing.
11	(Prasartkaew & Kumar, 2010)	Studied the mathematical modeling and simulation of a single effect LiBr–water system of absorption powered by biomass. The Performance of the entire system was evaluated based on a daily and monthly base.	Feasibility of solar–biomass-based air conditioning was determined by the results, for tropical locations of residential applications.
12	(Tsoutsos et al., 2010)	Customized simulation considering existence of a storage tank carried out about a LiBr-water absorption chiller	Noted that this 25kW with a 1500litres tank, the investment cost high and 11.5years as the payback period was without subsidy. Found it not viable for this very project.
13	(Mokhtar et al., 2010)	An analysis based on techno-economic factors for absorption chiller systems with respective solar collectors was carried out.	1. Large-scale industrial and commercial cooling plants were the most economical. 2. Storage tank sizing and heat rejection system selection, were determined to be fundamental contributors to the economic aspect of the system.
14	(Boopathi Raja & Shanmugam, 2012)	Carried out a study on how the minimum cost of a solar LiBr-water absorption cooling system can be obtained.	1. For a domestic setting, a single-stage LiBr–water absorption cooling system was more desired. 2. Evacuated tube and Flat plate collectors were found more economical than the rest of the other collectors.

			3. Optimized generator temperature ranges were 75-92°C and the temperature range at which evaporation takes place was 5–10°C.
15	(Lazzarin, 2014)	Comparison of various solar cooling techniques carried out with regards to how effective and economically feasible they are.	1. The solar PV cost was registered higher than that of solar thermal. 2. The cost of investment was relatively comparable for solar PV cooling systems and thermal systems for operation system capacity of 10kWh.
16	(Hang et al., 2013)	Comprehensive study about combined solar absorption systems for cooling and heating. Also, a system optimization procedure was carried out using TRNSYS simulation program.	Integrated systems are highly efficient and can be adopted for facilities that need either cooling, hot water or actual heating. The methodology can be optimized and applied for other solar energy solutions.
17	(Desideri et al., 2009)	Reviewed installation of solar cooling technology including flat plate solar energy collectors of 316m^2 area, a LiBr-H_2O chiller with a thermal storage of 30m^3.	1. The system performance was highly dependent on the site's solar environmental conditions as the main drive for the entire system. 2. The general installation cost of the system was fairly affordable.
18	(Zambrano et al., 2008)	Single-effect absorption cooling model developed, with flat plate collectors and a capacity of 35kW.	Successfully simulated the system with an achieved optimization recommending flat-plate collectors accompanied with a 2200-liter hot water storage tank. The investigational results were also in alignment with the ideal theoretical results.
19	(Ali et al., 2008)	An operation study was carried out for a 35.17kW LiBr-water	The utilized solar collector area was found to be 4.23m^2/kW. However, this area was found to be insufficient

		solar absorption chiller focusing on the performance for five years. The plant comprised of vacuum tube collectors, a $6.8m^3$ hot water tank, and a 134kW cooling tower.	and it was recommended that it is increased by the 25% of the initial area in order to improve the efficiency to required standard.
20	(Agyenim et al., 2010)	A study was conducted on a solar cooling system including vacuum tube collectors of area $12m^2$, a LiBr-H_2O absorption chiller of capacity 4.5kW, a 1000litre storage tank, together with a 6kW coil unit.	1. There was a proper demonstration of the effectiveness of cold storage. 2. The electrical and thermal COPs were measured to be 3.64 and 0.58, respectively. 3. To produce each kilowatt of cooling, a storage capacity of 180 to 250 liters is needed. 4. The delivered chilled water temperature of was 7°C.
21	(Said et al., 2012)	A detailed study was conducted about other related designs of solar absorption cooling technologies, investigating an NH_3-H_2O of 5kW capacity.	The best system of refrigeration includes thermal refrigerant storage with a high COP.
22	(Martínez et al., 2012)	17.6kW LiBr-H_2O single-stage absorption chiller was modeled and simulated using TRNSYS, using a system consisting a $38.4m^2$ flat-plate collector.	1. A 29% average of the incident solar energy was transferred to the thermal storage, from the solar collectors' surface. 2. The COP was 0.691.

2.9 Literature Conclusion

The studied literature indicates that single-effect absorption units are the most preferred and recommended systems for solar thermal cooling. The most used refrigerant solutions are Lithium Bromide-water (LiBr-H2O) and Ammonia-water (NH3-H2O) (Henderson et al., 2005). LiBr-H2O is recommended for cooling systems specifically designed for domestic thermal comfort, and chillers using NH3-H2O solutions are best designed for industrial purposes since they can produce a refrigerating effect at temperatures below zero (00C). For applications where above 00C cooling is needed, LiBr-H2O absorption chiller machines are preferred. However, the generator's temperature requirements range from 95-120°C for water-cooled absorption chillers, and this necessitates the use of concentrating collectors. For LiBr-water chillers, the system can handle temperatures that are a minimum of 70°C and this temperature can be obtained for LiBr-H2O absorption chillers by employing flat plate collectors, perfect for LiBr-H2O chillers and can help in cost cutting (Sreedevi et al., 2014).

When designing and operating a solar absorption cooling system, it's important to take into account the load profiles of the building, cooling needs, climate conditions, solar radiation specifications, site limitations, and energy supply conditions.

CHAPTER THREE: METHODOLOGY

3.1 Introduction

A review on how the research study objectives were addressed is presented in this chapter. It examined all the approaches used to collect and analyze the data regarding the design of a cooling system driven by solar thermal energy, for the cold storage facility at National Medical Stores.

3.2 Design of the Research

The research utilized both quantitative and qualitative methods for collecting all the data required to carry out the successful study.

Quantitative research methods were used to determine the respective solar thermal cooling equipment, design parameters and respective details, the system layouts, and the operation simulation of the designed system.

Qualitative research methods were used to analyze the cold storage operations and different types of thermal cooling systems that can satisfy the cold storage cooling needs.

3.3 Facility Details

The system cooling requirements were established from a comprehensive study and examination of the site to understand the structural details, the temperature requirements, and the cooling energy details.

3.4 Objective One: To Determine the Cooling Requirements of The Cold Storage System At NMS.

3.4.1 Cooling Load of the Facility

This is the rate at which heat is absorbed from a designated area to introduce and maintain a specific temperature and humidity. For this study, since there is an existing system in place, the requirements for cooling were already calculated using a simple procedure for cooling load calculation that is comprehensive but computes each element's impact to the total load requirements. This calculation procedure was considered for peak load design calculation.

According to the already installed cold room, the cold storage facility requires a cooling capacity of between 2^0C to 8^0C for it to deliver adequate, reliable, and appropriate cooling for the medicines stored in the facility.

Total prevailing Cooling load (Q_e), obtained from the installed system was therefore calculated using the formulae;

Apparent energy = rating of each unit x no of units (i)

Actual energy required = Apparent power x power factor (ii)

The power factor is 0.9 according to (Okoboi & Mawejje, 2016)

3.5 Objective Two: To Determine the Components and Parameters of the Cold Storage System.

3.5.1 System Design Layout

The system was designed to have the following major equipment components;

1. Solar collectors: the required collector area was calculated based on the amount of thermal energy required and flat plate solar collectors were selected to collect the required thermal energy.
2. Thermal storage system: A layered thermal storage tank was selected due to its special ability to maintain different temperatures between the different water layers in the tank (Sumathy et al., 2002). The storage tank size was based on the required thermal energy and the expected duration of cloudy days or periods without solar radiation.
3. Absorption chiller: The single-effect Lithium Bromide–Water based absorption chiller was selected (Assilzadeh et al., 2005), mainly because the desired cooling temperature requirements are above 0^0C and this system is recommended to handle this kind of requirement. This also takes into consideration the coefficient of performance (COP).
4. Fan Coil: Selection of the fan coil unit settled for the water-to-air fan coil, which consists of a coil and fan, was selected, receives chilled water, and uses it to remove heat from the air through heat transfer, and the air is used to cool the specified room (Rasuli & Torii, 2023).
5. Cooling tower: A cooling tower that uses evaporative heat rejection (Palomba et al., 2019) was selected to supply a cooling effect to the hot water in the chiller system as it is recycled for use. The cooling tower specifications were entirely dependent on the capacity of the absorption chiller.

The system layout was designed as shown in the figure 12, elaborating a view of the simple array of the respective components together.

The respective solar thermal cooling system components were designed independently and thereafter integrated to formulate the complete system,

The design layouts were created using the computer-based design software AUTOCAD based on the sizes and specifications determined from the respective calculations.

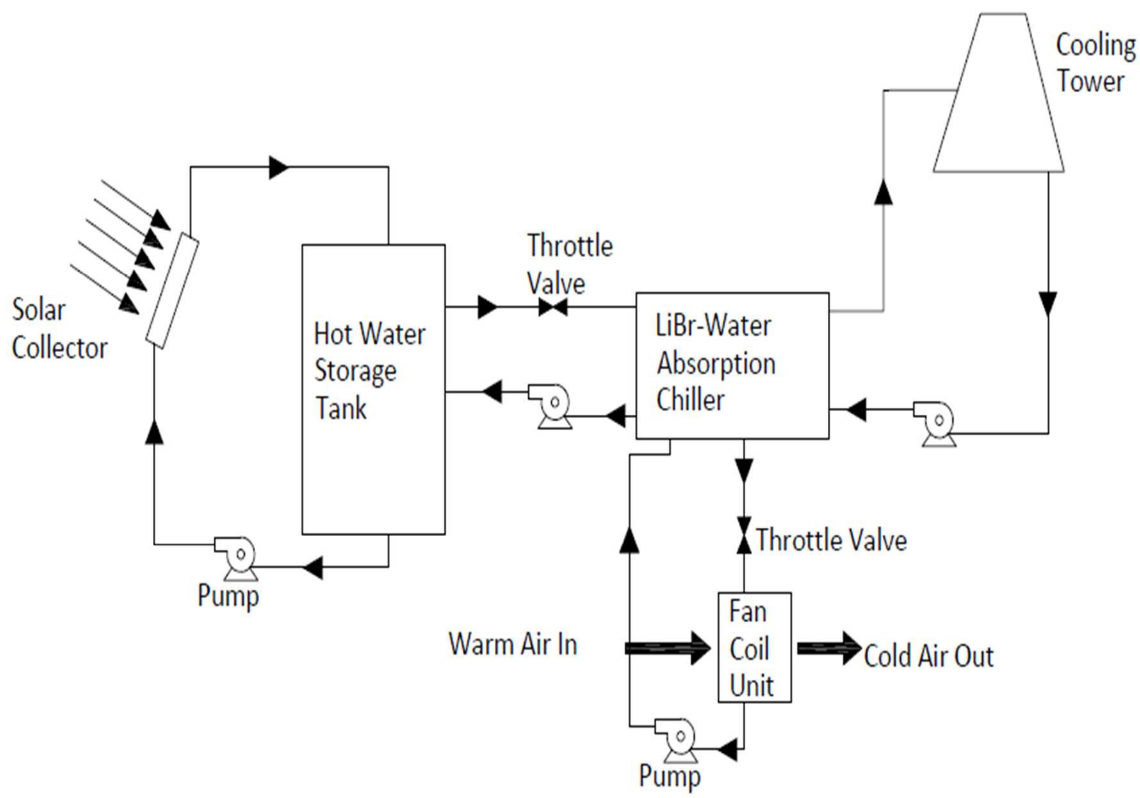

Figure 3.1: Layout of the Proposed Cooling System

The designed solar thermal cooling system is shown in the layout given in Figure 3.1

3.6 Objective Three: To Size the Components of the Solar Thermal Cooling System

3.6.1 The Absorption Chiller Design

The respective absorption chiller components and specifications were sized and calculated. The procedure of absorption cooling was plotted on a Pressure versus Temperature (P-T) diagram as below:

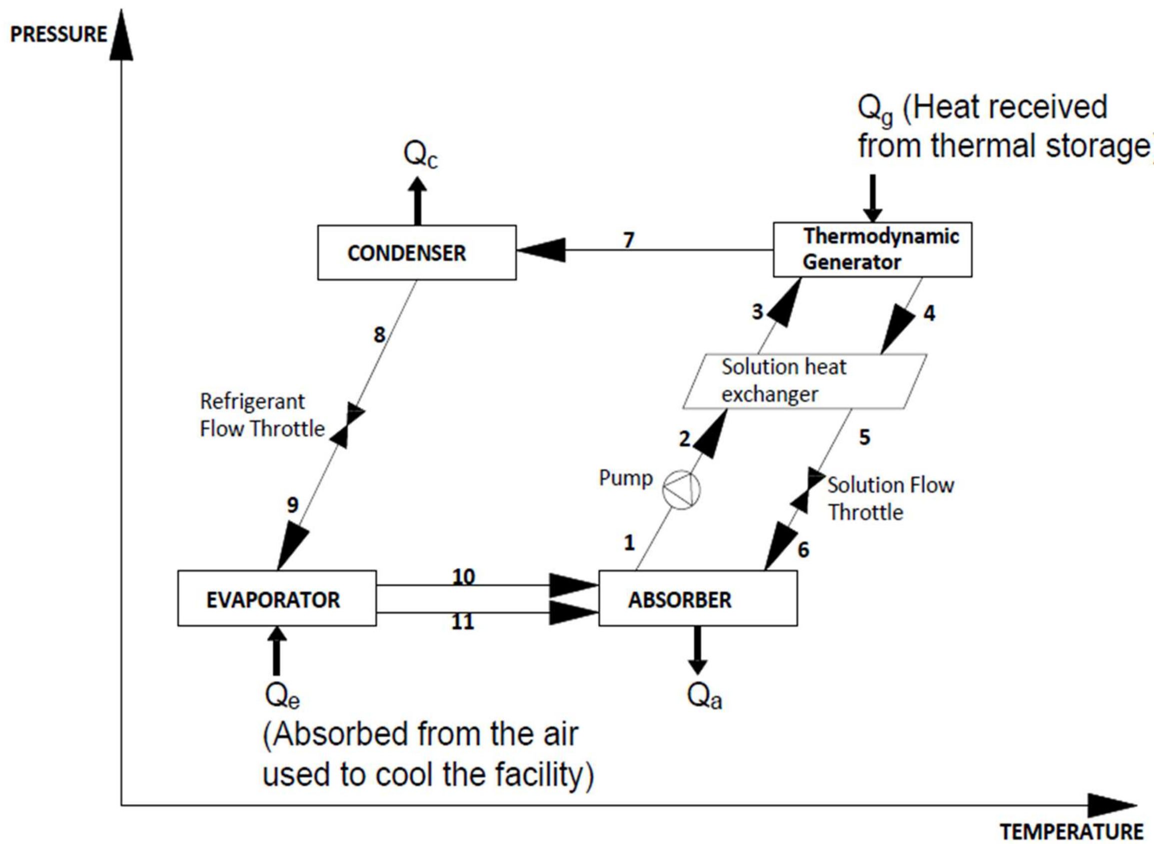

Figure 3.2: P-T diagram representing the LiBr-water absorption chiller model (Assilzadeh et al., 2005)

At the thermodynamic generator, the thermal input is received from the hot water storage tank, the LiBr-H_2O solution absorbs a Q_g quantity of heat and gives off a vaporized refrigerant. The heat absorbed evaporates the water in the LiBr-water refrigerant. The water vapor then goes through the condenser and releases a Q_c quantity of heat to be condensed to liquid form. The condensed water vapor refrigerant proceeds through a throttling device for pressure reduction as it proceeds to the evaporator and absorbs a Q_e quantity of heat from the fluid to be used for cooling. The absorber-evaporator section operates at very low pressures, hence decreasing the boiling point of water enabling it to be evaporated at low temperatures. The water vapor is thereafter passed on to the absorber and it gets absorbed by the highly concentrated LiBr-H_2O solution releasing a Q_a quantity of heat hence creating a less concentrated solution. This less concentrated solution at point 1 is pumped to the generator at high pressure through the solution heat exchanger, and the cycle is repeated to produce a cooling effect at the evaporator.

Once the water vapor (refrigerant) is sent to the condenser from the thermodynamic generator, the Lithium Bromide solution becomes highly concentrated (Point 4), and is sent to the heat exchanger and throttle valve to reduce its heat and pressure respectively. It is then sent to the absorber and the cycle is completed at the evaporator where the vaporized refrigerant is absorbed. To determine the respective component sizes and various parameters of the absorption chiller, some assumptions were put into account (ASHRAE, 2020);

1. The system was designed under steady-state conditions and water is used as the system refrigerant.
2. The pressure in the system doesn’t change apart from points where it moves through the throttle valves or the pump.
3. Points 1, 4, 8, and 11 are the only points at which saturated liquid is exhibited.
4. Point 10 is the only part where saturated vapor is exhibited.
5. Throttling is adiabatic, therefore doesn’t allow heat transfer in the system.

6. The pumping process is isentropic, hence keeping a constant entropy (degree of disorder or uncertainty of a system).

3.6.2 Absorption Chiller Model

Considering the parameters in the table. 2, and the assumptions considered for absorption chiller design, a mathematical model was performed for each component whereby; m = mass flow rate, Q = amount heat (thermal energy), h = enthalpy of the refrigerant solution, x = the mass fraction of the Lithium Bromide solution, W_p = minimum input work of the pump, P = pressure in the system, and v = specific volume of flow of the refrigerant.

3.6.3 Evaporator Model

Since the refrigerant in the evaporator is saturated water, and the temperature T_{10} was assumed to be 6^0C which is within the required temperature range, the saturation pressure and enthalpy at point 10 were obtained using steam tables. The refrigerant at 11 is saturated liquid whose enthalpy h_{11} was also obtained using steam tables.

At point 9, the enthalpy of the refrigerant was determined from the throttling process at the refrigerant flow, and therefore;

$$h_8 = h_9. \qquad \text{(iii)}$$

h_8 was calculated after determining the pressure at point 8.

At 4, the mass fraction of the solution X_4 is 60% LiBr, temperature of the saturated state is considered as 90^0C, the saturation pressure of the Lithium Bromide solution was obtained and h_4 was therefore obtained too.

After acquiring all the required values of enthalpy at the respective port connections to the evaporator, the mass and energy balances were utilized to give the mass flow of the refrigerant and the evaporator rate of heat transfer. The evaporator mass balance therefore is:

$$m_9 = m_{10} + m_{11} \quad \text{(iv)}$$

The evaporator energy balance is

$$Q_e = m_{10}h_{10} + m_{11}h_{11} - m_9h_9 \quad \text{(v)}$$

Since the output of the evaporator Q_e was known and m_{11} is $0.025m_{10}$, the mass flow rates were then calculated using equations (iv) and (v);

3.6.4 Absorber Model

After the values of m_{10} and m_{11} were acquired, mass balances were determined for the absorber;

$$m_1 = m_{10} + m_{11} + m_6 \quad \text{(vi)}$$

and

$$x_1m_1 = x_6m_6 \quad \text{(vii)}$$

Since x_1 and x_6 are inputs of the solution in equation (vii) therefore, m1 and m6 were then calculated.

The rate of heat transfer at the absorber was calculated using the values of enthalpy at the respective connected points. The enthalpy at point 1 was calculated using the input mass fraction (55%), since it's a saturated state liquid at a pressure similar to that at the evaporator P_1. At point 6, the enthalpy is given by the model from the throttling effect and;

$$h_6 = h_5 \quad \text{(viii)}$$

The enthalpy at 5 was calculated using the energy-balance model of the heat exchanger, and an adiabatic shell was assumed.

$$m_2h_2 + m_4h_4 = m_3h_3 + m_5h_5 \quad \text{(ix)}$$

At point 3, the temperature ($T_3 = 65^0C$) is an input value, and using the same value of the solution mass fraction since it is the same from point 1 to point 3, the enthalpy was therefore determined from steam tables. The pressure has a negligible effect on the enthalpy of the subcooled liquid, and hence, the saturated value at the same temperature and mass fraction can be a suitable approximation. The enthalpy at point 2 was obtained using the isentropic pump model.

The absorption chiller pump work (W_p) was obtained from the equation;

$$W_p = m_1 v_1 (p_2 - p_1) \quad \text{(x)}$$

In equation (x), the assumption is that the liquid solution's specific volume v (m^3/kg), doesn’t change significantly from 1 to 2. The specific volume of the LiBr-H_2O mixture was obtained using steam tables as seen in the appendix.

Equation (ix) was also used to attain the enthalpy value at point 5 (h_5), and the temperature T_5 at that point was determined using the enthalpy value.

Therefore, the final energy balance at the absorber was obtained by;

$$Q_a = m_{10}h_{10} + m_{11}h_{11} + m_6h_6 - m_1h_1 \quad \text{(xi)}$$

3.6.5 Thermodynamic Generator Model

Heat input to the thermodynamic generator (Q_g) was calculated using the energy balance equation;

$$Q_g = m_4h_4 + m_7h_7 - m_3h_3 \quad \text{(xii)}$$

At point 7, the enthalpy was determined using steam tables, since $T_7 = 85^0C$. Superheated water vapor exists at this point and therefore the enthalpy h_7 was determined from steam tables since the pressure and temperature were known.

3.6.6 Condenser Model

The thermal energy at the condenser was calculated using the energy balance equation;

$$Q_c = m_7(h_7 - h_8) \qquad \text{(xiii)}$$

3.6.7 System Coefficient of Performance (C.O.P)

The C.O.P of the system was calculated using the formula;

$$C.O.P = \frac{Qc}{Qg} \qquad \text{(xiv)}$$

3.6.8 Solar Collector Model

The design of the area of the solar collectors involved consideration of factors such as the location of the facility and system efficiency requirements. In the layout of the absorption chiller, a supply of heat is required at the thermodynamic generator from the solar collectors. The amount of hot water coming through was determined by the general area of the solar collector which determines how much thermal energy is collected and passed on as hot water. For calculation of the total area of the collector, both the heat amount for absorption supplied by the collectors, and the amount of heat being received at the surface of the collectors must be known. For typical solar collectors, the optimum tilt angle (Q_t) was obtained by adding the latitude of the site to 10^0 in the northern hemisphere since that's where the site is located. So, the tilt angle at Kajjansi is obtained by;

$$\Theta_t = \text{latitude}+10 \qquad \text{(xv)}$$

3.6.9 Solar Radiation

The available solar radiation data for three years; 2018 – 2020 was analyzed to obtain the average daily received radiation.

$$\text{Average monthly irradiation} = \frac{\text{Total horizontal monthly irradiations}}{\textit{Total number of months in 3years}}$$

$$\text{Average daily irradiation} = \frac{\text{Average monthly irradiation}}{30\,days}$$

Therefore, the average radiation received at the collectors was obtained by:

$$= \frac{\text{Average daily irradiation}}{\text{Average number of sun hours}} \qquad \text{(xvi)}$$

Considering 55% to be the recommended efficiency of flat plate solar collectors (Henderson et al., 2005 & Mahesh, 2017), to supply the required amount of thermal energy to fire the absorption chiller at the generator, the quantity of solar thermal energy to be collected at the flat plate collectors was therefore calculated from the formula;

$$= \frac{\text{Qg}}{efficiency(\%)}$$

The required collector area was therefore calculated using the equation;

$$= \frac{\text{Solar heat to be absorbed by the collector}}{\textit{Solar radiation}} \qquad \text{(xvii)}$$

3.6.10 Volume of the Thermal Storage

From the literature review, (Qu et al., 2010) concluded that for optimal solutions, the volume of the hot water storage tank ought to be within the range of 0.01 to $0.08m^3/m^2$. It is also recommended by (Agyenim et al., 2010), that the higher value ($0.08m^3/m^2$) should be taken for ideal design scenarios and to optimize the thermal energy storage and delivery during times when there might not be solar radiation, and also during the night.

The thermal storage tank volume was therefore obtained using the formula;

$$V = \text{Specific Volume x Area of the solar collectors} \quad \text{(xviii)}$$

3.7 Objective 4: To perform a Simulation of the Solar Thermal Cooling System

3.7.1 Design Simulation.

The simulation is necessary for this project to ascertain the performance of the designed system. Transient System Simulation Software (TRNSYS) was applied, and each component's characteristics, specifications, and parameters were input.

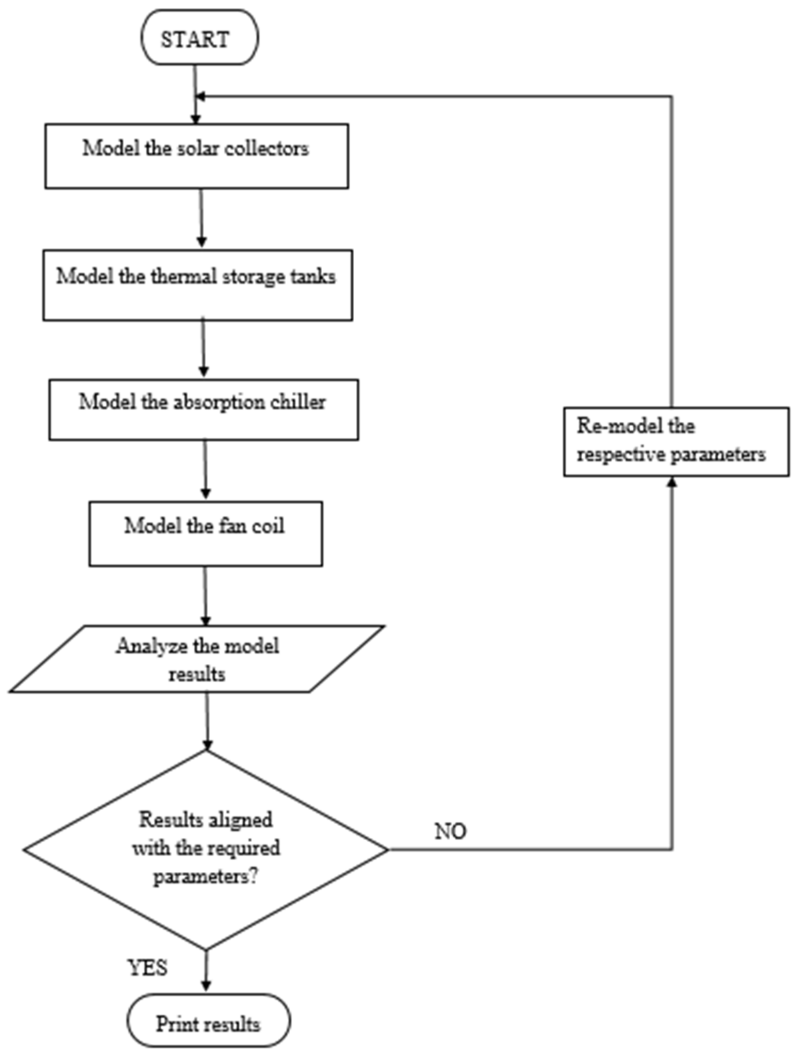

Figure 3.3: Flow model for simulating the selected components

The respective equipment was simulated as follows;

- **i.** Solar collector: the collector models were implemented within the simulation software, specifying the collector parameters based on the manufacturer's data and performance characteristics.
- **ii.** Heat transfer fluid: the system was modeled considering the fluid's heat transfer properties and the impact of fluid flow rates.
- **iii.** Thermal storage: the thermal storage was integrated into the system considering the properties of the storage materials, charging and discharging rates, and thermal losses.
- **iv.** Absorption chiller: the absorption chiller was incorporated into the simulation by specifying mainly the performance characteristics, and C.O.P curves.
- **v.** The fan coil: the fan coil was incorporated in the simulation considering the heat transfer and cooling rates.
- **vi.** Cooling tower: the heat rejection rate and fluid flow parameters were considered for the tower parameters.

All the respective components were then integrated into an interconnected system within the simulation environment ensuring that the interactions and feedback loops between the respective components were accurately represented.

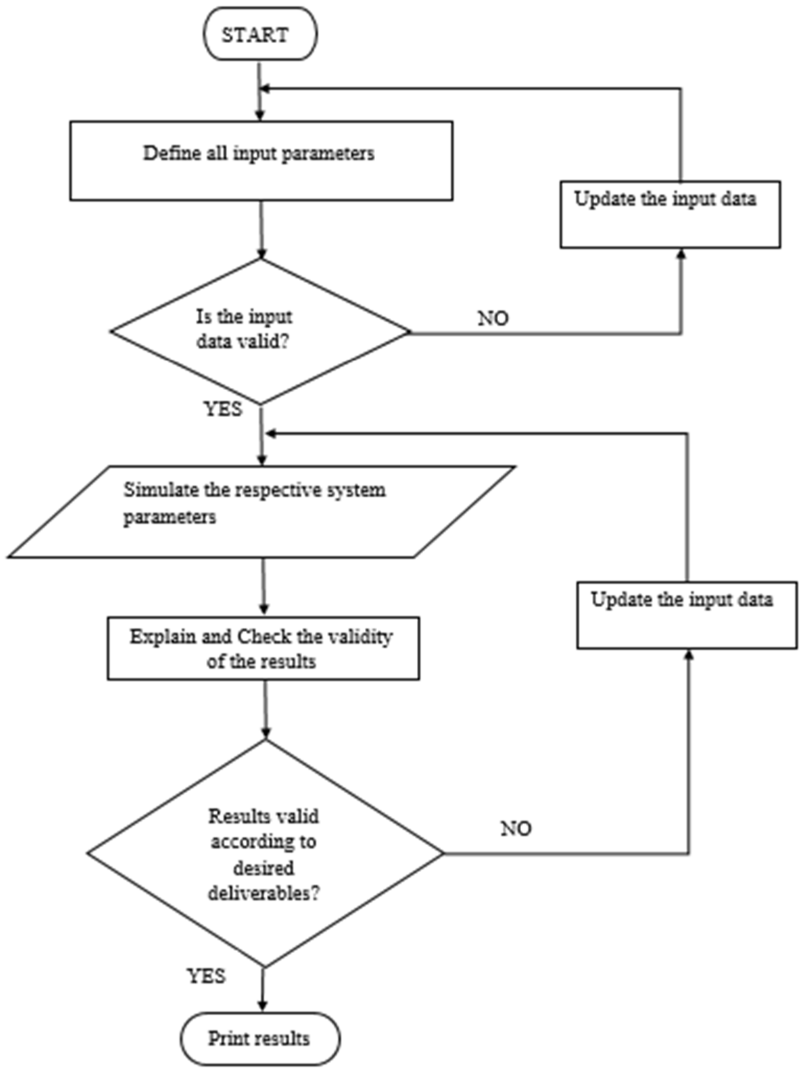

Figure 3.4: Flow model for simulating the designed system

The simulation's primary and boundary conditions, including the system's starting state, control set points, and all external influences, were defined before running the simulation.

The simulation was then executed, allowing the software to calculate the system’s behavior under specified conditions. The results from the simulation were obtained and analyzed to evaluate the operation details of the system for example cooling capacity, C.O.P, and energy efficiency.

A sensitivity analysis was conducted to understand how variations in different parameters would impact the overall system performance and opportunities for system optimization were considered, for example optimizing control strategies, collector orientations, or thermal storage sizing.

CHAPTER FOUR: RESULTS AND DISCUSSION

4.1 Introduction

This chapter presents the solar thermal cooling system design and simulation findings. It elaborates on the solar cooling system design process which involved a detailed consideration of various components and calculations to ensure that the system meets its requirements for efficiency and effectiveness. This involved analysis of factors such as solar energy input, absorption chiller design, and overall system performance to achieve the desired cooling outcome.

4.2 Objective One: To Determine the Cooling Requirements of the Cold Storage System at NMS.

4.2.1 Facility Details

The cold storage facility is located inside a warehouse, properly built up using sandwich panels to contain the cold temperature conditions in the facility and completely limit external warm air and heat from entering the storage. The cold storage system is in operation for is 24 hours therefore the cooling equipment runs both day and night. The facility covers a floor area of 746.2m^2 with a wall height of 3.55m.

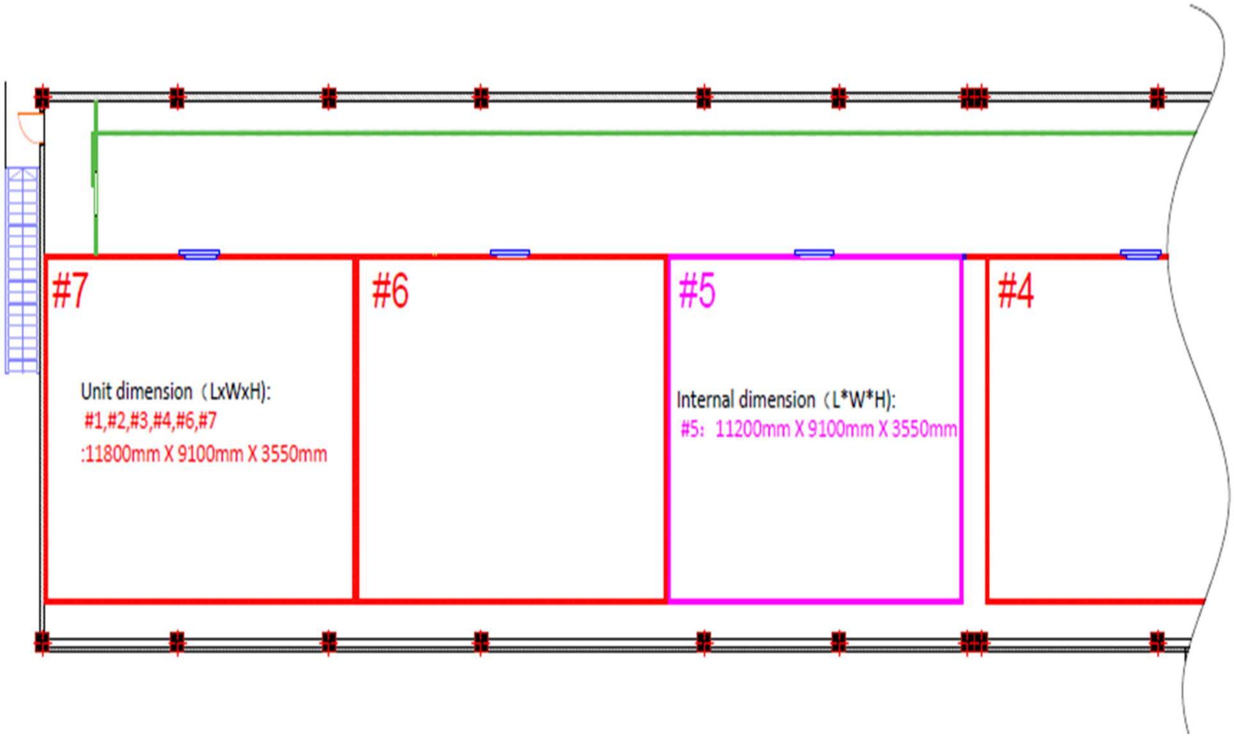

Figure 4.1: Structural Layout and Dimensions of the Cold-rooms

Figure 4.2: The existing system with some medications in storage

4.2.2 Cooling Requirements

Cooling requirements were determined mainly to ascertain that the initial existing design was done accurately to be sure that the cooling system designed would be sufficient since the design specifications are based on the existing system.

Cooling load calculations included the collection and processing of various respective data including the respective space heat gains and space cooling loads.

4.2.2.1 Heat Gains Experienced in the Facility

Facility heat acquisition is the rate at which thermal energy is accumulated in a building structure or the amount of heat produced inside the facility. Heat accumulation can be registered through different modes;

1. Through windows and transparent surfaces
2. Walls floors and roofs exposed to any form of solar radiation
3. From people, lights, and other appliances in the facility
4. Transfer of energy through vents and infiltrations from outdoors.

In this case, however, all these options for heat gain are already catered for since the facility is already designed and installed for cold storage, with sandwich panels, and doesn't allow any form of heat gain into the cold storage air space.

4.2.3 Cooling Load of the Faculty

This is the rate at which heat is absorbed from a designated area in order to introduce and maintain a specific temperature and humidity. The effect of cooling at any respective instant depends on the prevailing ambient temperature, which is determined by the heat accumulation during previous hours in addition to the prevailing heat accumulation.

For this study, since an existing system is in place, the requirements for cooling were already calculated using a simple procedure for cooling load calculation that is comprehensive but computes each element's impact to the total load requirements. This calculation procedure was considered for peak load design calculation.

According to the already installed cold room, the cold storage facility requires a cooling capacity of between 2^0C to 8^0C for it to deliver adequate, reliable and appropriate cooling for the medicines stored in the facility.

Total prevailing Cooling load (Q_e), obtained from the installed system is therefore;

Q_e = Total wattage required from the installed system

Apparent energy = 50kVA x 7units

= 350kVA

Actual energy required = Apparent energy x power factor

= *(350 x 0.9) kW*

= 315kW

Therefore, Q_e = 315kW

The Peak cooling demand for the installed cold storage system is 315kW and this can also be presented as 1,074,824 BTU/hr where 1kW equals 3412 BTU/hr.

.

4.3 Objective Two: To Determine the Components and Parameters of the Solar Thermal Cooling System.

The respective solar thermal cooling system components were designed independently and thereafter integrated to formulate the complete system.

The design layouts were created using the computer-based design software AUTOCAD, based on the sizes and specifications determined from the respective calculations.

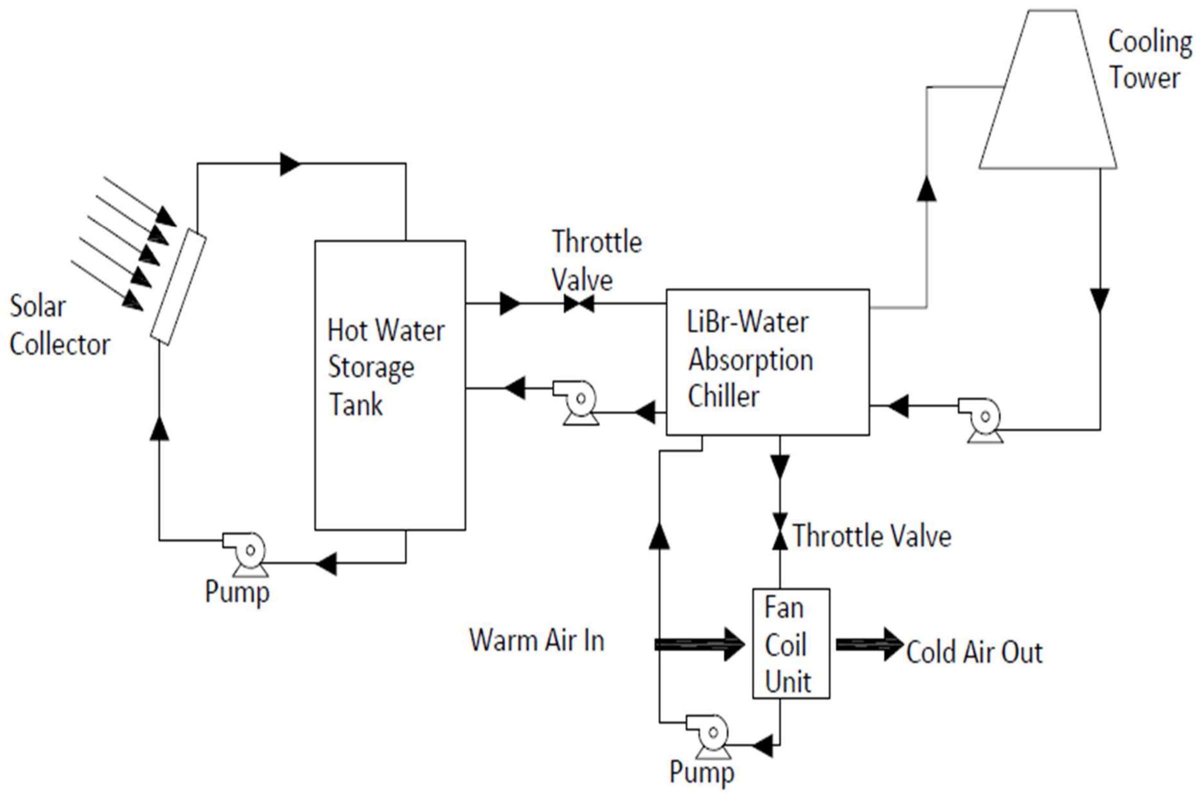

Figure 4.3: Layout of the proposed solar thermal cooling system

The components of the designed solar thermal cooling system are shown in the layout given in figure 4.3

4.4 Objective 4: To Size the Components of the Solar Thermal Cooling System

4.4.1 The Absorption Chiller Analysis

Some parameters were considered as shown in the table below which were considered for the design analysis.

Table 4.1: Parameters considered in designing and modeling the single effect LiBr-H_2O absorption chiller (ASHRAE, 2020).

S/No	Parameter	Symbol	Value
1	System capacity	Q_e	315kW
2	Evaporator temperature	T_{10}	6^0C
3	Thermodynamic Generator exit solution temperature	T_4	90^0C
4	Concentration of the weak solution	X_1	55% LiBr
5	Strong concentration of the solution	X_4	60% LiBr
6	Thermodynamic Generator inlet solution temperature	T_3	65^0C
7	Vapor exit temperature at the thermodynamic Generator	T_7	85^0C
8	Liquid carry-over from the evaporator	m_{11}	$0.025m_{10}$

Considering the parameters in the table. 2 above, and the assumptions considered for absorption chiller design, a mathematical calculations were performed for each component and the respective results were obtained.

4.4.1.1 Evaporator Analysis

The refrigerant in the evaporator is saturated water, and its temperature T_{10} was taken to be 6^0C, the pressure of saturation at point 10 is obtained using steam tables as 0.934kPa and the enthalpy is obtained as 2511.8kJ/kg. The refrigerant at point 11 is saturated liquid and its enthalpy h_{11} is obtained as 23.5kJ/kg. At point 9, the enthalpy of the refrigerant is obtained from the process of throttling at the refrigerant flow, and therefore $h_8 = h_9$. h_8 is calculated after the pressure at point 8 has been obtained. At point 4, the mass fraction of the solution X_4 is 60% LiBr, and the saturated state temperature is 90^0C, the Lithium Bromide solution gives 9.66kPa as the saturation pressure and h_4 is therefore 212.2kj/kg. Since the pressure at points 4 and 8 is equal, therefore $h_8 = h_9 = 185.3$kJ/kg.

After acquiring all the required values of enthalpy at the respective port connections to the evaporator, the energy and mass equations were utilized to give the refrigerant's mass flow and the rate of heat transfer of the evaporator.

The evaporator mass balance therefore is:

$$m_9 = m_{10} + m_{11}$$

The evaporator energy balance is

$$Q_e = m_{10}h_{10} + m_{11}h_{11} - m_9h_9$$

Since; Q_e = 315kW, $m_{11} = 0.025m_{10}$, h_{10} = 2511.8kj/kg, h_9 = 185.3kj/kg, h_{11} = 23.5kj/kg, $m_9 = (m_{10} + 0.025m_{10})$

$$315 = m_{10} \text{ x } 2511.18 + 0.025m_{10} \text{ x } 23.5 - (m_{10} + 0.025m_{10}) \text{ x } 185.3$$

$$m_{10} = 0.1357\text{kg/s}$$

$$m_{11} = 0.025 \text{ x } 0.1357 = 0.0034\text{kg/s}$$

$$m_9 = 0.1357 + 0.0034 = 0.1393\text{kg/s}$$

4.4.1.2 Absorber Analysis

After the m_{10} and m_{11} values were acquired, the masses were determined for the absorber;

$m_1 = m_{10} + m_{11} + m_6$

$m_1 = 0.1357 + 0.0034 + m_6$

and

$x_1 m_1 = x_6 m_6$

Since $x_1 = 0.55$ and $x_6 = 0.60$

$m_1 = 0.6m_6 \div 0.55$

$0.6m_6 = 0.1393 + m_6 \times 0.55$

$m_6 = 2.786$kg/s

$m_1 = (0.6 \times 2.786) \div 0.55 = 3.0393$kg/s

The rate of heat transfer at the absorber was calculated using the values of enthalpy at the respective connected points. The enthalpy at point 1 was calculated using the input mass fraction (55%), assuming it's a saturated state liquid at a pressure similar to that at the evaporator

$P_1 = 0.934$kPa.

This enthalpy value $h_1 = 83$kJ/kg.

At point 6, the enthalpy is given by the model from the throttling effect and;

$h_6 = h_5$

At point 3, the temperature ($T_3 = 65^0$C) is an input value, and using the same value of the solution mass fraction since it is the same from point 1 to point 3, the enthalpy at this point was determined to be 145.4kJ/kg. The enthalpy at point 2 was obtained using the isentropic pump model. The pump work input (W_p) was obtained from the equation

$W_p = m_1 v_1 (p_2 - p_1)$

In the above equation, the assumption is that the liquid solution's specific volume v_1 (m^3/kg), doesn't change significantly from points 1 to 2. The LiBr-H_2O solution's specific volume was obtained using steam tables as seen in the appendix. Since all the variables were known, the pump power was calculated as;

$$W_p = 3.0393 \text{ x } 0.6271(9.66 - 0.934) = 16.63W.$$

The enthalpy at point 5 was calculated using the balance model of the solution heat exchanger energy, and an adiabatic shell was assumed.

$$m_2h_2 + m_4h_4 = m_3h_3 + m_5h_5$$

$$(3.0393x83) + (2.786x212.2) = (3.0393x145.4) + (2.786xh_5)$$

$$h_5 = 144.13kj/kg$$

The temperature at that point was determined using the enthalpy value and is $T_5 = 54.8^0C$.

Also, $h_6 = h_5 = 144.13kj/kg$

Therefore, the final energy balance at the absorber was obtained by using the formula;

$$Q_a = m_{10}h_{10} + m_{11}h_{11} + m_6h_6 – m_1h_1$$

$Q_a = (0.1884x2511.8) + (0.0034x23.5) + (3.0393x144.13) – (2.3151x83) = 490.22kW$

4.4.1.3 Thermodynamic Generator Analysis

The amount of heat delivered to the Thermodynamic generator (Q_g) was calculated using the energy balance equation;

$$Q_g = m_4h_4 + m_7h_7 – m_3h_3$$

At point 7, the enthalpy was determined using steam tables, since $T_7 = 85^0C$. At this point, it is superheated water vapor and the enthalpy $h_7 = 2659.03kJ/kg$ was therefore determined from steam tables since the pressure and temperature were known.

Therefore;

$$Q_g = (2.786x212.2) + (0.1393x2659) - (3.0393x145.4) = 519.69kW$$

4.4.1.4 Condenser Analysis

The thermal energy at the condenser was calculated using the energy balance equation;

$$Q_c = m_7(h_7 - h_8)$$

$$Q_c = 0.1931\ (2659 - 185.3) = 344.59kW$$

4.4.1.5 System Coefficient of Performance (C.O.P)

$$C.O.P = \frac{Qc}{Qg} = \frac{315}{519.69} = 0.606$$

Table 4.2: Calculated parameters of the LIBr-H_2O absorption chiller

Specified Point	h (kJ/kg)	m (kg/s)	P (kPa)	T (^{0}C)	X (% LiBr)
1	83	3.0393	0.9335	34.93	55
2	83	3.0393	9.661	34.93	55
3	145.41	3.0393	9.661	65	55
4	212.21	2.1786	9.661	90	60
5	144.13	2.1786	9.661	54.82	60
6	144.13	2.1786	0.9335	44.54	60
7	2659	0.1393	9.661	85	0
8	185.3	0.1393	9.661	44.3	0
9	185.3	0.1393	0.9335	6	0
10	2511.8	0.1357	0.9335	6	0
11	23.5	0.0034	0.9335	6	0

Table 4.3:Thermal energy specifications for the respective components of the absorption chiller

Component	Symbol	Quantity (kW)
Cooling capacity of the system (Evaporator delivery)	Q_e	315
Work input by the pump	W_p	0.0166
Heat dissipated to the environment by the absorber	Q_a	490.22
Thermal energy required by the generator	Q_g	519.69
Heat dissipated to the environment by the condenser	Q_c	344.59

The required cooling load was calculated and determined as 315kW, and thus the different absorption chiller components and specifications were sized and calculated. The process of absorption cooling was plotted on a Pressure versus Temperature (P-T) diagram below showing the energy requirements at the respective components:

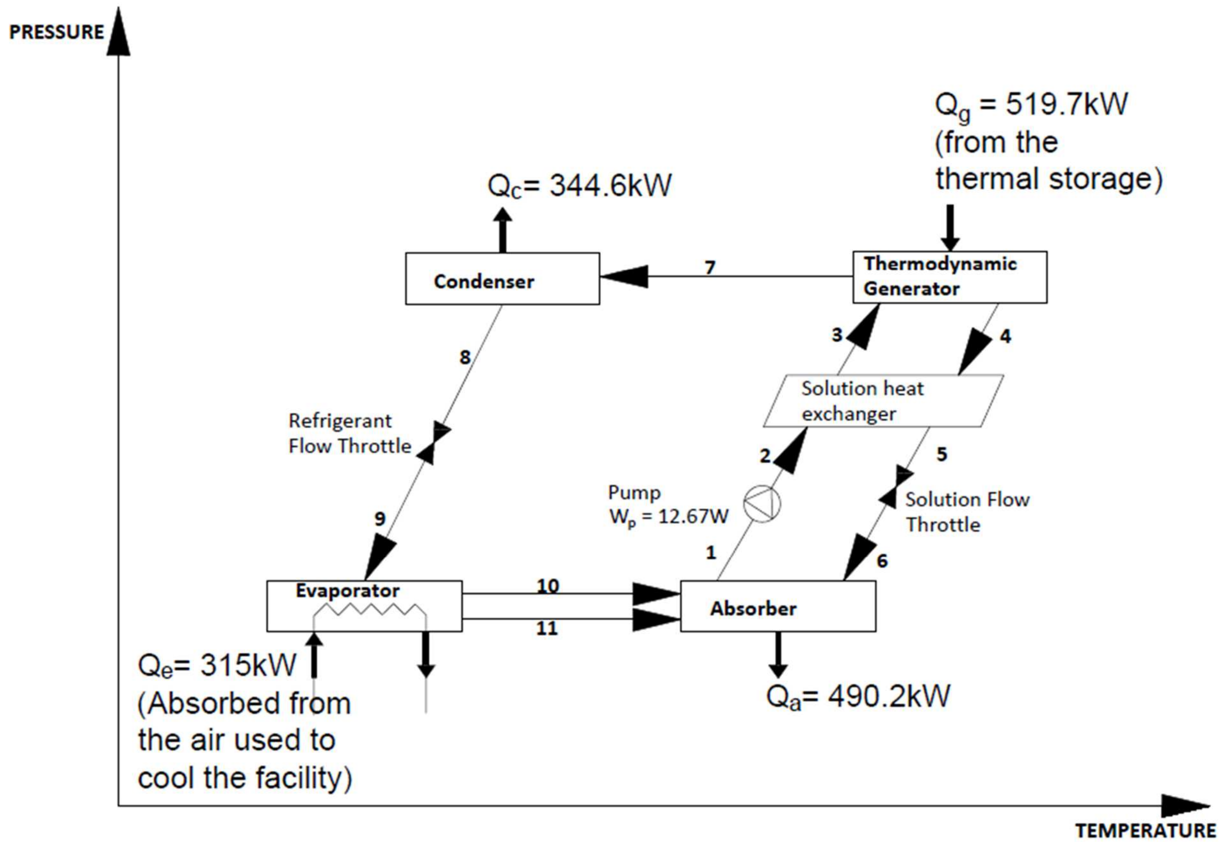

Figure 4.4: P-T diagram showing the calculated energies at the respective absorption chiller stages

At the thermodynamic generator, the thermal input is received from the hot water storage tank which receives the heat from the flat plate solar collectors, the LiBr-H_2O solution absorbs 519.7kW of heat, and the absorbed heat vaporizes the water in the LiBr-water refrigerant. The water vapor then goes through the condenser and releases a 434.6kW quantity of heat to be condensed to liquid form. The condensed water vapor refrigerant proceeds through a throttling device for pressure reduction as it proceeds to the evaporator, absorbing 315kW of heat from the fluid which is used to cool the cold storage facility as required. The absorber-evaporator section operates at very low pressures, hence decreasing the boiling point of water enabling it to be evaporated at low temperatures.

The vapor is thereafter passed on to the absorber being absorbed by the highly concentrated LiBr-H_2O solution releasing 490.2kW of heat hence creating a less concentrated solution. This less concentrated solution at point 1 is sent to the thermodynamic generator at high pressure passing through the solution heat exchanger, and the cycle is repeated to produce a cooling effect at the evaporator.

Once the water vapor (refrigerant) is sent to the condenser from the generator, the Lithium Bromide solution becomes highly concentrated (Point 4), and is passed in the solution heat exchanger and also the throttle valve to reduce its heat and pressure respectively. It is then sent to the absorber completing the cycle at the evaporator where the refrigerant vapor is absorbed.

4.4.2 Solar Collector Area Design

4.4.2.1 Tilt angle

For typical solar collectors, the optimum tilt angle (Q_t) was obtained by adding the latitude of the site to 10^0 in the northern hemisphere since that's where the site is located. So, the tilt angle at Kajjansi is obtained by;

$$\Theta_t = \text{latitude} + 10^0 = 0.3476+10^0 = 10.3476 = 10^o$$

4.4.2.2 Solar Radiation over Kajjansi, Kampala – Uganda

The available solar radiation data for three years; 2018 – 2020 was analyzed to obtain the average daily received radiation.

Table 4.4: Global Horizontal irradiation for Kajjansi (PV-GIS, 2024)

Month	2018	2019	2020
January	182.7	190.08	170.8
February	169.5	180.54	172.1
March	151.45	201.23	170.98
April	134.9	177.66	161.02
May	145.82	164.5	156.72
June	138.18	121.58	149.06
July	168.42	154.03	153.37
August	156.98	142.1	164.1
September	173.02	154.75	161.04
October	157.91	165.5	149.78
November	174.45	150.6	150.51
December	153.6	147.24	163.42

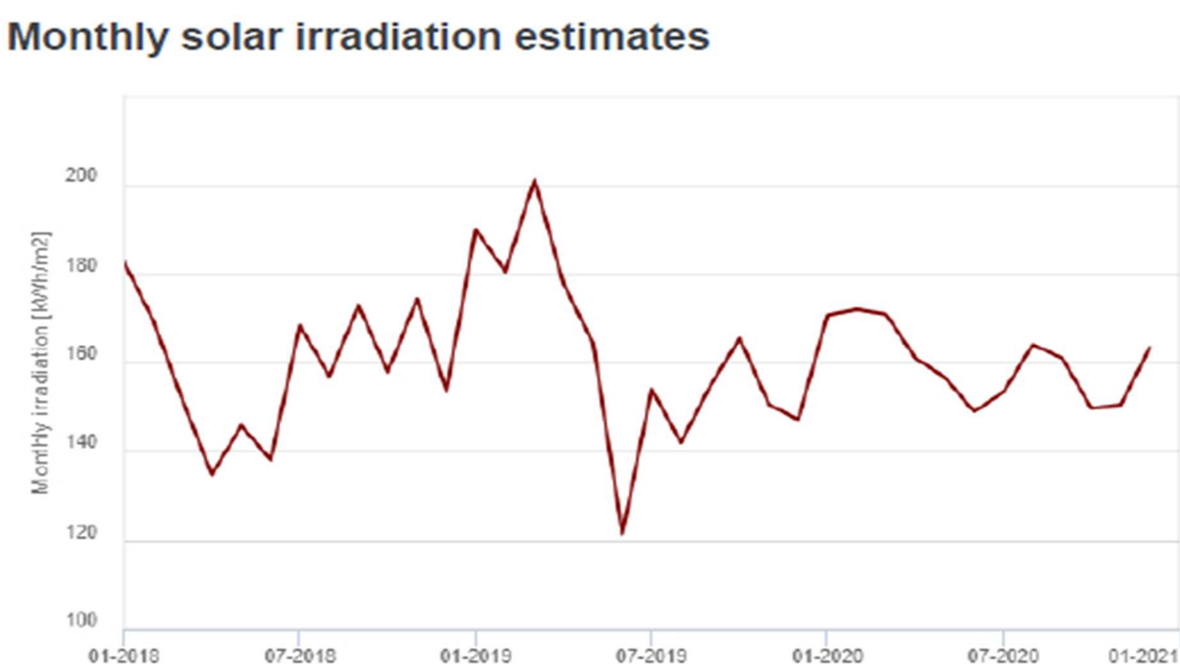

Figure 4.5: Graph of monthly solar irradiation estimates experienced in Kajjansi

Estimated average monthly irradiation = $\frac{\text{Total horizontal monthly irradiations}}{\textit{Total number of months in 3years}}$

$= 160.55 kWh/m^2$

Estimated average daily irradiation = $\frac{\text{Average monthly irradiation}}{30days}$

$=5.352 kWh/m^2$

Therefore, the average radiation received at the collectors is:

$= \frac{\text{Average daily irradiation}}{\text{Average number of sun hours}}$

$= \frac{5.352}{8}$

$= 0.669 kW/m^2 = 669 W/m^2$

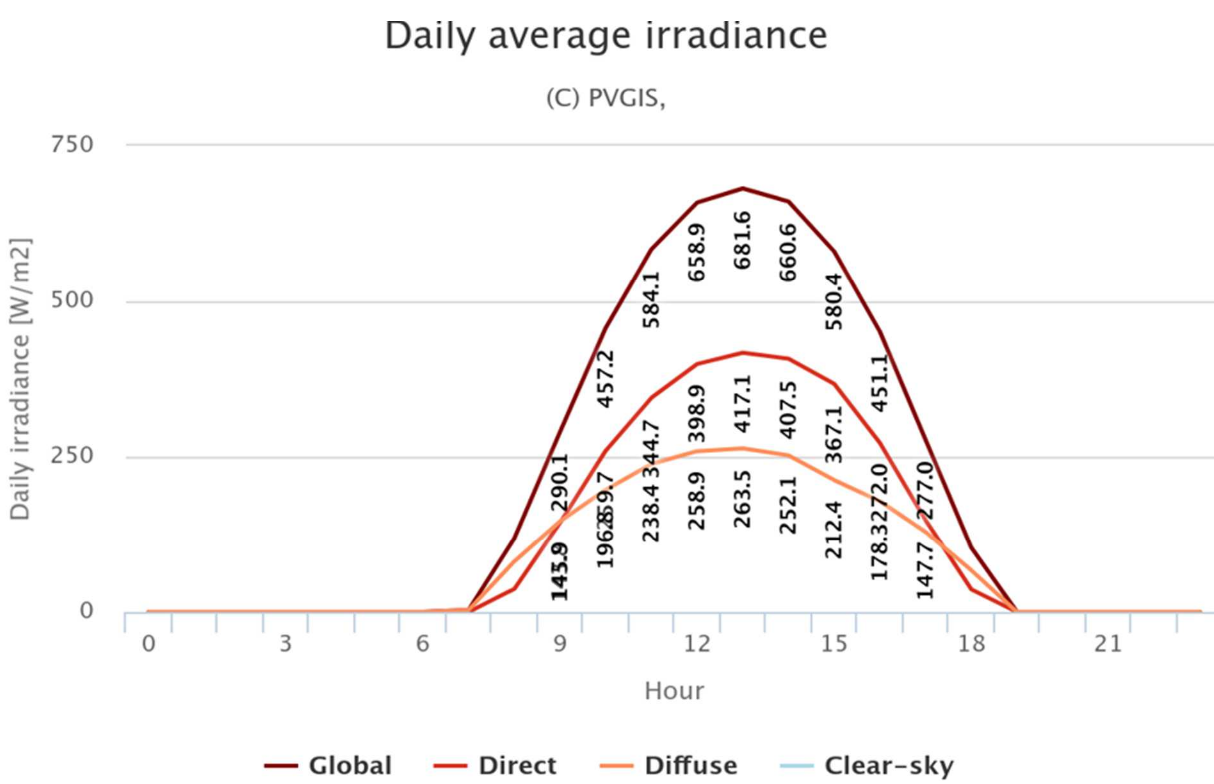

Figure 4.6: Graph of daily average solar irradiation experienced in Kajjansi (PV-GIS, 2024)

With a tilt angle of 10^0, at any surface of the solar collector around Kajjansi and considering an average number of sun hours as 8 hours, the solar radiation was obtained as $669W/m^2$. According to previous researchers 55% is considered the best efficiency of flat plate collectors based on the operation conditions (Mahesh, 2017) & (Kinnier, 1981), required to supply 627.13kW of solar energy to fire the absorption chiller at the generator, the quantity of solar thermal energy to be collected at the flat plate collectors can therefore be calculated from the formula;

$$= \frac{Qg}{efficiency(\%)}$$

$$= \frac{519.69}{0.55}$$

$$= 944.89kW$$

$$= 944{,}890W$$

The required collector area was therefore calculated as:

$$= \frac{\text{Solar heat to be absorbed by the collector}}{Solar\ radiation}$$

$$= \frac{994{,}890}{669}$$

$$= 1{,}487m^2$$

4.4.3 Hot Water Storage Volume

From the literature review, (Qu et al., 2010) concluded that for optimal solutions, the volume of the thermal storage tank ought to be within the 0.01 to $0.08m^3/m^2$ range. It is also recommended by (Agyenim et al., 2010), that the higher value ($0.08m^3/m^2$) should be taken for ideal design scenarios and to optimize the thermal energy storage and delivery during times when there might not be solar radiation, and also during the night.

The volume of the thermal storage tank volume was therefore calculated using the formula;

$$V = \text{Specific Volume x Area of the solar collectors}$$

$$= 0.08 \times 1487$$

$$= 118.96m^3$$

$$= 119m^3$$

4.5 Objective Four: To Perform a Simulation of the Solar Thermal Cooling System

4.5.1 Simulating the Designed Solar Cooling System

Transient System Simulation Program (TRNSYS) was used for simulating the designed solar thermal cooling system, according to Kampala - Uganda's climatic data.

4.5.1.1 Input Parameters

Tables 4.2 and 4.3 above, summarize the input properties and parameters of the respective cooling system components. The metrological weather and operation data were selected directly from the simulation software according to the site location in Kajjansi, Kampala – Uganda. The respective component parameters and variables were set up in the deck files according to the design model calculations. Some other parameters and specifications are ideal standard conditions as presented by (ASHRAE, 2020) for solar thermal cooling design exercises. The program was thereafter executed.

Table 4.5: Flat Plate Collector Parameters for TRNSYS Simulation

Parameter	Description	Value
b_o	Incidence angle modifier constant	0.1
C_{pc}	Collector fluid's specific heat (kJ/kg C)	4.19
G_{test}	Flow rate per unit area	54
a_o	Efficiency at interception	0.792
a_1	First-order coefficient of the efficiency (kJ/h m^2C)	23.994
e	Collector loop heat exchanger	None used
Optical mode		Incidence modifiers
Efficiency mode		$n\ v_s\ (T_i - T_a)l_T$

n = efficiency; T_i = collector fluid entrance temperature (^{0}C); T_a = ambient temperature; I_T = incident radiation (kJ/m^2 h)

4.5.1.2 Simulation Components Layout

The respective component models were accurately selected in TRNSYS and all their specifications and parameters were input, and the layout of the modeled system is as presented in the Fig 4.7.

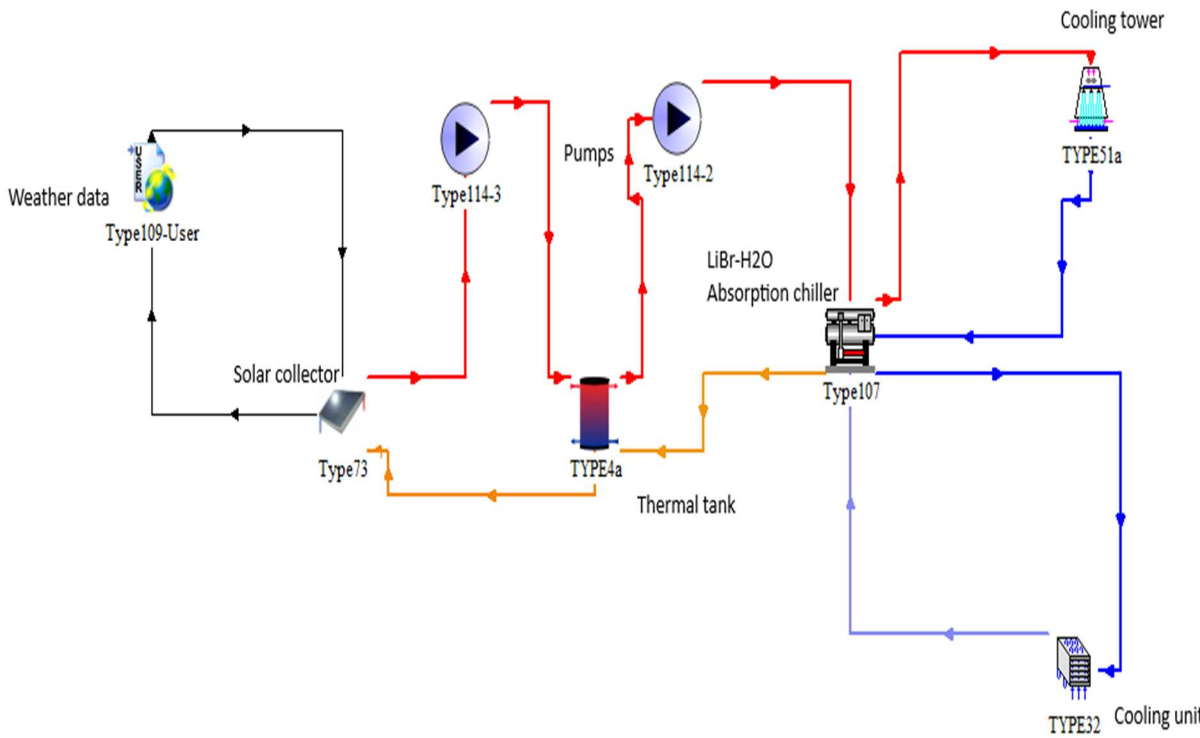

Figure 4.7: Layout of the component's assembly in TRNSYS software

4.5.1.3 Temperature Profile of the Major Components of the Solar Thermal Cooling System

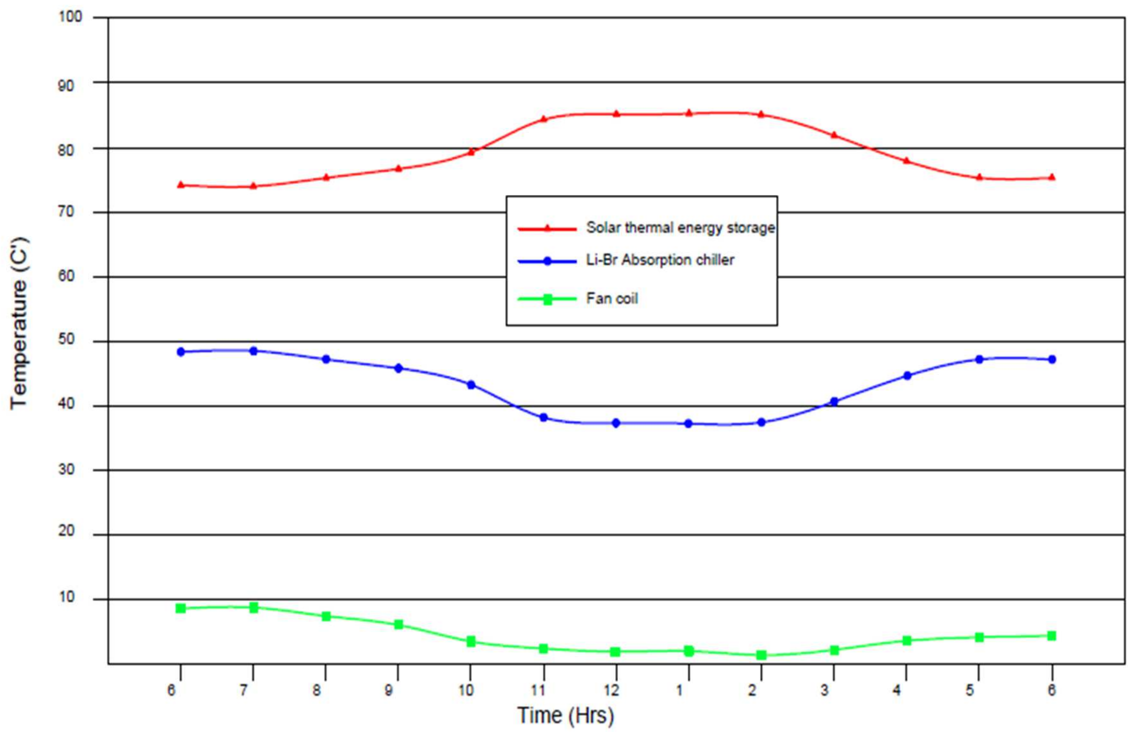

Figure 4.8 Temperature Profile of the Solar Thermal Cooling System

The temperature profile of the major components of the solar thermal cooling system is presented in figure 4.8, which elaborates the average temperature conditions of each of the respective sections in the system. The solar thermal storage registers a higher average temperature (between 70-80^0C) because it signifies the direct thermal energy harvested from the sun rays and stored in the thermal storage tank.

The Li-Br Absorption chiller registers a mid-range average operational temperature (between 30 - 50^0C) because it transforms thermal energy into a cooling effect as required for the purpose of the system.

The fan coil registers the lowest average working temperatures (between 0-10^{0}C) simply because it works with fluids that have already been chilled by the absorption chiller and are ready to cool the cold storage facility at a temperature between 2-8^{0}C as required.

4.5.1.3 System Performance

The system energy flows are shown in the fig. 4.9, which gives the basic performance that is obtained considering the final specifications of the system.

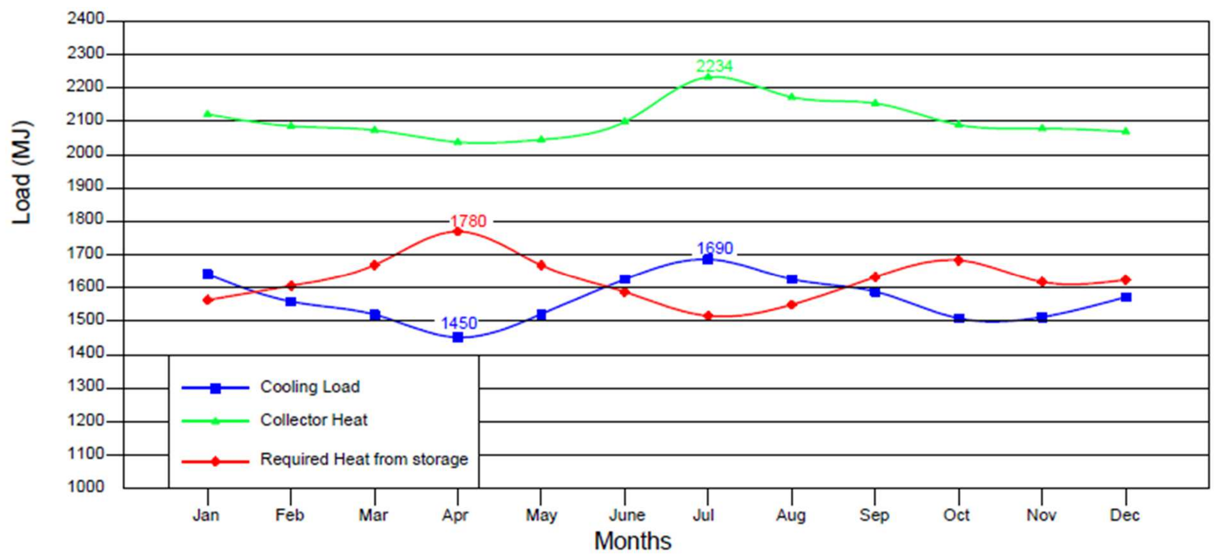

Figure 4.9: System Energy Flows

The maximum heat energy generated monthly using the solar collector system was 2,234 MJ in July. The maximum amount of heat required from the thermal storage by the cooling requirements is 1780 MJ, and this occurs in April when the solar collector supplies energy at its lowest; 1,450 MJ. The highest cooling energy supplied monthly by the solar system is 1,690 MJ, also in July, when the solar collector system collects the maximum amount of thermal energy. Throughout the monthly operations, the minimum cooling load is 1450 MJ (402.8 kWh), which is above the required 1134 MJ (315 kWh) to provide the necessary cooling to the facility. This therefore justifies that the designed system will at all incidences provide more cooling than required hence is viable for the operations. The simulation also included a coefficient of friction which was 0.667 which lies within the ASHRAE recommended C.O.P, (0.6 - 0.8). This also justifies the viability of the designed and simulated solar thermal cooling system since it lies within the recommended ad acceptable range.

4.6 Final System Specifications

The specifications of the final system model determined from the simulation and calculations are presented in the table 4.6.

Table 4.6: Specifications of the final system

Item	Value/Type
Capacity of unit	315kWh
Type of collector	Flat Plate
Area of collector	$1487m^2$
Collector tilt angle	10^0
Thermal storage tank size	$119m^3$
Thermostat setting temperature	85^0C

4.7 Economic Analysis

This included an establishment of the bill of quantities of the designed solar cooling system which would be used for implementation of the system. Some of the materials are locally available. However, other materials have to be imported for example materials for the chiller and hot water storage systems. In addition, the economic analysis of the system was presented to justify its competitive advantage over the alternate system that is powered using the national grid.

4.7.1 Bill of Materials and Quantities

This was mainly implemented to establish the initial investment cost, which involved the total project cost derived from the respective component materials, the indirect costs and the costs of labour and installation. The designed cooling system was divided into five major sections according to its major components and costs were determined for each of the respective sections and is presented in the table 4.6.

Table 4.7: Summarized Bill of Materials and Quantities of the Solar Thermal Cooling System

S/No.	Description	Unit	Qty	Unit Cost (UGX)	Amount (UGX)
1	Flat Plate Solar collectors with pump, piping accessories and brackets for mounting	No	1	104,120,000	104,120,000
2	Hot water storage tank with pump and all accessories	No	1	478,212,000	478,212,000
3	Absorption Chiller with all components installed	No	1	572,000,000	572,000,000
4	Cooling tower with its accessories	No	1	314,673,000	314,673,000
5	Fan Coil Unit with its piping	No	1	4,394,130	74,394,130
	TOTAL COST				**1,543,399,130**

Labour = 30% x total equipment cost = 463,019,739 UGX

Therefore, the total project cost = 1,543,399,130 + 463,019,739 = 2,006,418,869

Maintenance cost = 5% x Total project cost

= 0.05 x 2,006,418,869

= 100,320,943 UGX

Indirect costs = 10% x total project cost

= 0.1 x 2,006,418,869

= 200,641,886 UGX

The total cost of investment for the solar cooling system therefore was calculated as;

= 2,006,418,869 + 200,641,886 + 100,320,943

= 2,307,381,699 UGX

4.7.2 Simple Payback Period

The payback period was calculated based on the initial cost of investment of the cooling system and how much savings would be realized if the system was installed.

Payback period = (Total cost of investment) / (Monthly saving from grid power)

Monthly saving = daily saving x 31days

= 3,491,208 x 31

= 108,227,448 UGX

Therefore, payback period = 2,307,381,699 ÷ 108,227,448

= 21.32months

The payback period of 21.32 months indicates that if the facility switches from using grid power to the designed solar thermal cooling system, it would take less than 2 years for national medical stores to break even. This therefore means after 21.32 months with the designed cooling system in place, National Medical Stores will have saved an amount equal to the investment of installing the cooling system and will after that operate under profits. Therefore, the system would be cost effective for National Medical Stores once installed since it will eventually bring down the high expense generated by running the existing cold storage cooling system using the national grid.

CHAPTER FIVE: CONCLUSION AND RECOMMENDATIONS

Conclusions derived from the results obtained and discussed are presented in this section. It also includes recommendations made to the industry and areas to be considered for further study.

5.1 Conclusion

A method that utilizes solar thermal energy for cooling the cold storage facility at National Medical Stores. The system was modelled and simulated using TRNSYS simulation software, using weather information for Kampala. The final designed system of capacity 315kW and a coefficient of performance of 0.606 consists of a 1,487m^2 flat plate collector sloped at 10^0 , a 119m^3 thermal storage tank, and can deliver a cooling effect to 6^0C which is within the required range of 2 – 8^0C. The designed solar thermal cooling system, therefore, presents a viable alternate solution to electric cooling systems, especially for areas with high solar irradiance.

For the system to achieve uninterrupted operation, a thermal storage unit should be incorporated to keep a constant provision of heat to the absorption chiller at the generator to increase the system's reliability.

The solar thermal cooling system would create a monthly saving of 108,227,448UGX which would have been paid for grid power charges and would then be paid back in a period of 21.32 months, and this would make a quick return on investment and hence justify that the system is very viable for the operation.

Even though this study's findings are customized to the system at National Medical Stores, the author believes similar results can equally be obtained for facilities in other areas that have enough solar radiation. However, before designing and confirming any respective type of cooling system to install at any facility, customization should be done according to the prevailing weather conditions, operation needs, and any other requirements for it to work as desired.

Finally, given the issue of global pollution resulting from operations, machinery or equipment that use fossil fuels, the significance of adopting solar power for cooling activities, even when the overall benefits are minimal, should be extensively utilized.

5.2 Recommendations

It is recommended therefore, that National Medical Stores installs the designed system to solve the problem of the high cost of operation of the cold storage facility resulting from using the national grid power, since the designed system results prove viability. However a prototype needs to be implemented first before the final system can be put into consideration.

More training and sensitization should be carried out to inform the communities about the benefits of solar systems especially to provide cooling and heating for building spaces, but also hot water to be used for bathrooms and laundry activities.

The government should support and encourage the adoption of solar thermal systems since they utilize clean energy and do not contribute to carbon content in the atmosphere and pollution.

5.3 Areas for Further Research

Research about designs customized to generate both cooling and heating solutions to be utilized by facilities like academic institutions, hospitals, and others.

REFERENCES

Agyenim, F., Knight, I., & Rhodes, M. (2010). Design and experimental testing of the performance of an outdoor LiBr/H2O solar thermal absorption cooling system with a cold store. *Solar Energy*, *84*(5), 735–744. https://doi.org/10.1016/j.solener.2010.01.013

Alazazmeh, A. J., & Mokheimer, E. M. (2015). Review of Solar Cooling Technologies. *Journal of Applied Mechanical Engineering*, *04*(05). https://doi.org/10.4172/2168-9873.1000180

Ali, A. H. H., Noeres, P., & Pollerberg, C. (2008). Performance assessment of an integrated free cooling and solar powered single-effect lithium bromide-water absorption chiller. *Solar Energy*, *82*(11). https://doi.org/10.1016/j.solener.2008.04.011

Antonia et al. (2021). Renewable Energy Sources. *Renewable and Appropriate Energy Laboratory*.

ASHRAE. (2020). 2020 ASHRAE Handbook SI Edition. In *Ashrae Handbook, Fundamentals*.

ASHRAE handbook. (2017). 2017 ASHRAE handbook : fundamentals. In *ASHRAE handbook : fundamentals*.

Assilzadeh, F., Kalogirou, S. A., Ali, Y., & Sopian, K. (2005). Simulation and optimization of a LiBr solar absorption cooling system with evacuated tube collectors. *Renewable Energy*, *30*(8), 1143–1159. https://doi.org/10.1016/j.renene.2004.09.017

Boopathi Raja, V., & Shanmugam, V. (2012). A review and new approach to minimize the cost of solar assisted absorption cooling system. In *Renewable and Sustainable Energy Reviews* (Vol. 16, Issue 9, pp. 6725–6731). https://doi.org/10.1016/j.rser.2012.08.004

Delač, B., Pavković, B., & Lenić, K. (2018). Design, monitoring and dynamic model development of a solar heating and cooling system. *Applied Thermal Engineering*, *142*, 489–501. https://doi.org/10.1016/j.applthermaleng.2018.07.052

Delahunt, J. (2016). Knowledge - Refrigeration Cycle. *Building Engines*.

Desideri, U., Proietti, S., & Sdringola, P. (2009a). Solar-powered cooling systems: Technical and economic analysis on industrial refrigeration and air-conditioning applications. *Applied Energy*, *86*(9). https://doi.org/10.1016/j.apenergy.2009.01.011

Desideri, U., Proietti, S., & Sdringola, P. (2009b). Solar-powered cooling systems: Technical and economic analysis on industrial refrigeration and air-conditioning applications. *Applied Energy*, *86*(9). https://doi.org/10.1016/j.apenergy.2009.01.011

Dudin, M. N., Frolova, E. E., Protopopova, O. V., Mamedov, A. A., & Odintsov, S. V. (2019). Study of innovative technologies in the energy industry: Nontraditional and renewable energy sources. *Entrepreneurship and Sustainability Issues*, *6*(4). https://doi.org/10.9770/jesi.2019.6.4(11)

Eicker, U., & Pietruschka, D. (2009). Design and performance of solar-powered absorption cooling systems in office buildings. *Energy and Buildings*, *41*(1), 81–91. https://doi.org/10.1016/j.enbuild.2008.07.015

Florides, G. A., Kalogirou, S. A., Tassou, S. A., & Wrobel, L. C. (2003). Design and construction of a LiBr-water absorption machine. *Energy Conversion and Management*, *44*(15), 2483–2508. https://doi.org/10.1016/S0196-8904(03)00006-2

Ganguly, A. (2016). Solar thermal-photovoltaic powered potato cold storage-Conceptual design and performance analyses Author links open overlay panel Dipankar N. *Applied Energy*, *165*, 308–317. https://doi.org/10.1016/j.apenergy.2015.12.070Get

Gevorkian, P. (2012). Large-Scale Solar Power Systems. In *Large-Scale Solar Power Systems*. https://doi.org/10.1017/cbo9781139226608

Gupta, A. (2014). *DESIGN AND SIMULATION OF SOLAR THERMAL COOLING AND HEATING SYSTEM*. https://www.researchgate.net/publication/265441476

Hang, Y., Du, L., Qu, M., & Peeta, S. (2013). Multi-objective optimization of integrated solar absorption cooling and heating systems for medium-sized office buildings. *Renewable Energy*, *52*, 67–78. https://doi.org/10.1016/j.renene.2012.10.004

Henderson, G., Barnard, N., Jaunzens, D., Armstrong, J., Butler, D., & Dr. Leventhall, G. (2005). Guide B: Heating, Ventilating, Air Conditioning and Refrigeration (CIBSE Guide B). In *CIBSE*.

International Energy Agency, The World Bank, Sarah, F., The World Bank, Rahut, D. B., Mottaleb, K. A., Ali, A., Aryal, J., Smith, B., Soares, P. M. M., Brito, M. C., Careto, J. A. M., Shahsavari, A., Akbari, M., Lee, J. T., Callaway, D. S., IRENA, Pirard, E., Hatem, T. M., … Essia, U. (2021). Global Solar Atlas. In *Renewable and Sustainable Energy Reviews* (Vol. 90, Issue March).

Kinnier, R. J. (1981). AIR-TO-AIR ENERGY-RECOVERY EQUIPMENT. *Plant Engineering (Barrington, Illinois)*, *35*(6).

Lazzarin, R. M. (2014). Solar cooling: PV or thermal? A thermodynamic and economical analysis. *International Journal of Refrigeration*, *39*. https://doi.org/10.1016/j.ijrefrig.2013.05.012

Mahesh, A. (2017). Solar collectors and adsorption materials aspects of cooling system. In *Renewable and Sustainable Energy Reviews* (Vol. 73, pp. 1300–1312). Elsevier Ltd. https://doi.org/10.1016/j.rser.2017.01.144

Mahmood Aljamali, N., Hussain Khadum, L., & Abdulhussein Jabbar, A. (n.d.). Applications of Cooling Systems via Using Solar Thermal-Photovoltaic Panels: Literature Review. *Journal of Thermal Energy System*, *6*. www.matjournals.com

Marcos, J. D., Izquierdo, M., & Parra, D. (2011). Solar space heating and cooling for Spanish housing: Potential energy savings and emissions reduction. *Solar Energy*, *85*(11), 2622–2641. https://doi.org/10.1016/j.solener.2011.08.006

Martínez, P. J., Martínez, J. C., & Lucas, M. (2012). Design and test results of a low-capacity solar cooling system in Alicante (Spain). *Solar Energy*, *86*(10), 2950–2960. https://doi.org/10.1016/j.solener.2012.06.030

Ministry of Energy and Mineral Development. (2019). *Energy Report*.

Mokhtar, M., Ali, M. T., Bräuniger, S., Afshari, A., Sgouridis, S., Armstrong, P., & Chiesa, M. (2010). Systematic comprehensive techno-economic assessment of solar cooling technologies using location-specific climate data. *Applied Energy*, *87*(12), 3766–3778. https://doi.org/10.1016/j.apenergy.2010.06.026

Monné, C., Alonso, S., Palacín, F., & Serra, L. (2011). Monitoring and simulation of an existing solar powered absorption cooling system in Zaragoza (Spain). *Applied Thermal Engineering*, *31*(1), 28–35. https://doi.org/10.1016/j.applthermaleng.2010.08.002

Montagnino, F. M. (2017). Solar cooling technologies. Design, application and performance of existing projects. *Solar Energy*, *154*, 144–157. https://doi.org/10.1016/j.solener.2017.01.033

National Medical Stores. (2023). *National Medical Stores Annual Energy Report* .

Okoboi, G., & Mawejje, J. (2016). The impact of adoption of power factor correction technology on electricity peak demand in Uganda. *Journal of Economic Structures*, *5*(1). https://doi.org/10.1186/s40008-015-0034-3

Palacín, F., Monné, C., & Alonso, S. (2011). Improvement of an existing solar powered absorption cooling system by means of dynamic simulation and experimental diagnosis. *Energy*, *36*(7), 4109–4118. https://doi.org/10.1016/j.energy.2011.04.035

Palomba, V., Wittstadt, U., Bonanno, A., Tanne, M., Harborth, N., & Vasta, S. (2019). Components and design guidelines for solar cooling systems: The experience of ZEOSOL. *Renewable Energy*, *141*, 678–692. https://doi.org/10.1016/j.renene.2019.04.018

Perez-Lombard, L., Ortiz, J., & Maestre, I. R. (2011). The map of energy flow in HVAC systems. *Applied Energy*, *88*(12). https://doi.org/10.1016/j.apenergy.2011.07.003

Prasartkaew, B., & Kumar, S. (2010). A low carbon cooling system using renewable energy resources and technologies. *Energy and Buildings*, *42*(9), 1453–1462. https://doi.org/10.1016/j.enbuild.2010.03.015

Qu, M., Yin, H., & Archer, D. H. (2010). A solar thermal cooling and heating system for a building: Experimental and model based performance analysis and design. *Solar Energy*, *84*(2), 166–182. https://doi.org/10.1016/j.solener.2009.10.010

Rasuli, M. A., & Torii, S. (2023). A Review on Solar Air Conditioning Systems. *Article in Journal of Sustainable Energy Revolution*, *4*(1), 1–13. https://doi.org/10.37357/1068/jser/4.1.01

Said, S. A. M., El-Shaarawi, M. A. I., & Siddiqui, M. U. (2012). Alternative designs for a 24-h operating solar-powered absorption refrigeration technology. *International Journal of Refrigeration*, *35*(7), 1967–1977. https://doi.org/10.1016/j.ijrefrig.2012.06.008

Sreedevi, A., Kaul, A., & Radhika, K. (2014). Modeling and simulation of an HVAC system for energy analysis and management of commercial buildings. *Proceedings of International Conference on Circuits, Communication, Control and Computing, I4C 2014*. https://doi.org/10.1109/CIMCA.2014.7057787

Sumathy, K., Huang, Z. C., & Li, Z. F. (2002). *SOLAR ABSORPTION COOLING WITH LOW GRADE HEAT SOURCE-A STRATEGY OF DEVELOPMENT IN SOUTH CHINA †* (Vol. 72, Issue 2). www.elsevier.com/locate/solener

Tsoutsos, T., Aloumpi, E., Gkouskos, Z., & Karagiorgas, M. (2010). Design of a solar absorption cooling system in a Greek hospital. *Energy and Buildings*, *42*(2), 265–272. https://doi.org/10.1016/j.enbuild.2009.09.002

Xu, Z. Y., & Wang, R. Z. (2017). Simulation of solar cooling system based on variable effect LiBr-water absorption chiller. *Renewable Energy*, *113*, 907–914. https://doi.org/10.1016/j.renene.2017.06.069

Zambrano, D., Bordons, C., Garcia-Gabin, W., & Camacho, E. F. (2008). Model development and validation of a solar cooling plant. *International Journal of Refrigeration*, *31*(2). https://doi.org/10.1016/j.ijrefrig.2007.05.007

Zhai, X. Q., Qu, M., Li, Y., & Wang, R. Z. (2011). A review for research and new design options of solar absorption cooling systems. In *Renewable and Sustainable Energy Reviews* (Vol. 15, Issue 9, pp. 4416–4423). https://doi.org/10.1016/j.rser.2011.06.016

APPENDICES

Appendix A: Steam Tables

TABLE B.2 Saturated Water: Pressure Table 6

P kPa, MPa	T °C	$\hat{v}_l$ m^3/kg	$\hat{v}_v$ m^3/kg	$\hat{u}_l$ kJ/kg	$\Delta\hat{u}_{lv}$ kJ/kg	$\hat{u}_v$ kJ/kg	$\hat{h}_l$ kJ/kg	$\Delta\hat{h}_{lv}$ kJ/kg	$\hat{h}_v$ kJ/kg	$\hat{s}_l$ kJ/kg K	$\Delta\hat{s}_{lv}$ kJ/kg K	$\hat{s}_v$ kJ/kg K
0.6113	0.01	0.001000	206.132	0	2375.3	2375.3	0.00	2501.3	2501.3	0	9.1562	9.1562
1.0	6.98	0.001000	129.208	29.29	2355.7	2385.0	29.29	2484.9	2514.2	0.1059	8.8697	8.9756
1.5	13.03	0.001001	87.980	54.70	2338.6	2393.3	54.70	2470.6	2525.3	0.1956	8.6322	8.8278
2.0	17.50	0.001001	67.004	73.47	2326.0	2399.5	73.47	2460.0	2533.5	0.2607	8.4629	8.7236
2.5	21.08	0.001002	54.254	88.47	2315.9	2404.4	88.47	2451.6	2540.0	0.3120	8.3311	8.6431
3.0	24.08	0.001003	45.665	101.03	2307.5	2408.5	101.03	2444.5	2545.5	0.3545	8.2231	8.5775
4.0	28.96	0.001004	34.800	121.44	2293.7	2415.2	121.44	2432.9	2554.4	0.4226	8.0520	8.4746
5.0	32.88	0.001005	28.193	137.79	2282.7	2420.5	137.79	2423.7	2561.4	0.4763	7.9187	8.3950
7.5	40.29	0.001008	19.238	168.76	2261.7	2430.5	168.77	2406.0	2574.8	0.5763	7.6751	8.2514
10.0	45.81	0.001010	14.674	191.79	2246.1	2437.9	191.81	2392.8	2584.6	0.6492	7.5010	8.1501
15.0	53.97	0.001014	10.022	225.90	2222.8	2448.7	225.91	2373.1	2599.1	0.7548	7.2536	8.0084
20.0	60.06	0.001017	7.649	251.35	2205.4	2456.7	251.38	2358.3	2609.7	0.8319	7.0766	7.9085
25.0	64.97	0.001020	6.204	271.88	2191.2	2463.1	271.90	2346.3	2618.2	0.8930	6.9383	7.8313
30.0	69.10	0.001022	5.229	289.18	2179.2	2468.4	289.21	2336.1	2625.3	0.9439	6.8247	7.7686
40.0	75.87	0.001026	3.993	317.51	2159.5	2477.0	317.55	2319.2	2636.7	1.0258	6.6441	7.6700
50.0	81.33	0.001030	3.240	340.42	2143.4	2483.8	340.47	2305.4	2645.9	1.0910	6.5029	7.5939
75.0	91.77	0.001037	2.217	384.29	2112.4	2496.7	384.36	2278.6	2663.0	1.2129	6.2434	7.4563
0.100	99.62	0.001043	1.6940	417.33	2088.7	2506.1	417.44	2258.0	2675.5	1.3025	6.0568	7.3593
0.125	105.99	0.001048	1.3749	444.16	2069.3	2513.5	444.30	2241.1	2685.3	1.3739	5.9104	7.2843
0.150	111.37	0.001053	1.1593	466.92	2052.7	2519.6	467.08	2226.5	2693.5	1.4335	5.7897	7.2232
0.175	116.06	0.001057	1.0036	486.78	2038.1	2524.9	486.97	2213.6	2700.5	1.4848	5.6868	7.1717
0.200	120.23	0.001061	0.8857	504.47	2025.0	2529.5	504.68	2202.0	2706.6	1.5300	5.5970	7.1271
0.225	124.00	0.001064	0.7933	520.45	2013.1	2533.6	520.69	2191.3	2712.0	1.5705	5.5173	7.0878
0.250	127.43	0.001067	0.7187	535.08	2002.1	2537.2	535.34	2181.5	2716.9	1.6072	5.4455	7.0526
0.275	130.60	0.001070	0.6573	548.57	1992.0	2540.5	548.87	2172.4	2721.3	1.6407	5.3801	7.0208
0.300	133.55	0.001073	0.6058	561.13	1982.4	2543.6	561.45	2163.9	2725.3	1.6717	5.3201	6.9918
0.325	136.30	0.001076	0.5620	572.88	1973.5	2546.3	573.23	2155.8	2729.0	1.7005	5.2646	6.9651
0.350	138.88	0.001079	0.5243	583.93	1965.0	2548.9	584.31	2148.1	2732.4	1.7274	5.2130	6.9404
0.375	141.32	0.001081	0.4914	594.38	1956.9	2551.3	594.79	2140.8	2735.6	1.7527	5.1647	6.9174
0.40	143.63	0.001084	0.4625	604.29	1949.3	2553.6	604.73	2133.8	2738.5	1.7766	5.1193	6.8958
0.45	147.93	0.001088	0.4140	622.75	1934.9	2557.6	623.24	2120.7	2743.9	1.8206	5.0359	6.8565
0.50	151.86	0.001093	0.3749	639.66	1921.6	2561.2	640.21	2108.5	2748.7	1.8606	4.9606	6.8212
0.55	155.48	0.001097	0.3427	655.30	1909.2	2564.5	655.91	2097.0	2752.9	1.8972	4.8920	6.7892
0.60	158.85	0.001101	0.3157	669.88	1897.5	2567.4	670.54	2086.3	2756.8	1.9311	4.8289	6.7600
0.65	162.01	0.001104	0.2927	683.55	1886.5	2570.1	684.26	2076.0	2760.3	1.9627	4.7704	6.7330
0.70	164.97	0.001108	0.2729	696.43	1876.1	2572.5	697.20	2066.3	2763.5	1.9922	4.7158	6.7080

TABLE B.4 Superheated Water Vapor

$P = 10$ kPa

T °C	$\hat{v}$ m³/kg	$\hat{u}$ kJ/kg	$\hat{h}$ kJ/kg	$\hat{s}$ kJ/kg K
sat	14.674	2437.9	2584.6	8.1501
50	14.869	2443.9	2592.6	8.1749
100	17.196	2515.5	2687.5	8.4479
150	19.513	2587.9	2783.0	8.6881
200	21.825	2661.3	2879.5	8.9037
250	24.136	2736.0	2977.3	9.1002
300	26.445	2812.1	3076.5	9.2812
400	31.063	2968.9	3279.5	9.6076
500	35.679	3132.3	3489.0	9.8977
600	40.295	3302.5	3705.4	10.1608
700	44.911	3479.6	3928.7	10.4028
800	49.526	3663.8	4159.1	10.6281
900	54.141	3855.0	4396.4	10.8395
1000	58.757	4053.0	4640.6	11.0392
1100	63.372	4257.5	4891.2	11.2287
1200	67.987	4467.9	5147.8	11.4090
1300	72.603	4683.7	5409.7	11.5810

$P = 50$ kPa

T °C	$\hat{v}$ m³/kg	$\hat{u}$ kJ/kg	$\hat{h}$ kJ/kg	$\hat{s}$ kJ/kg K
sat	3.240	2483.8	2645.9	7.5939
100	3.418	2511.6	2682.5	7.6947
150	3.889	2585.6	2780.1	7.9400
200	4.356	2659.8	2877.6	8.1579
250	4.821	2735.0	2976.0	8.3555
300	5.284	2811.3	3075.5	8.5372
400	6.209	2968.4	3278.9	8.8641
500	7.134	3131.9	3488.6	9.1545
600	8.058	3302.2	3705.1	9.4177
700	8.981	3479.5	3928.5	9.6599
800	9.904	3663.7	4158.9	9.8852
900	10.828	3854.9	4396.3	10.0967
1000	11.751	4052.9	4640.5	10.2964
1100	12.674	4257.4	4891.1	10.4858
1200	13.597	4467.8	5147.7	10.6662
1300	14.521	4683.6	5409.6	10.8382

$P = 100$ kPa

T °C	$\hat{v}$ m³/kg	$\hat{u}$ kJ/kg	$\hat{h}$ kJ/kg	$\hat{s}$ kJ/kg K
sat	1.6940	2506.1	2675.5	7.3593
100	1.6958	2506.6	2676.2	7.3614
150	1.9364	2582.7	2776.4	7.6133
200	2.1723	2658.0	2875.3	7.8342
250	2.4060	2733.7	2974.3	8.0332
300	2.6388	2810.4	3074.3	8.2157
400	3.1026	2967.8	3278.1	8.5434
500	3.5655	3131.5	3488.1	8.8341
600	4.0278	3301.9	3704.7	9.0975
700	4.4899	3479.2	3928.2	9.3398
800	4.9517	3663.5	4158.7	9.5652
900	5.4135	3854.8	4396.1	9.7767
1000	5.8753	4052.8	4640.3	9.9764
1100	6.3370	4257.3	4890.9	10.1658
1200	6.7986	4467.7	5147.6	10.3462
1300	7.2603	4683.5	5409.5	10.5182

$P = 200$ kPa

T °C	$\hat{v}$ m³/kg	$\hat{u}$ kJ/kg	$\hat{h}$ kJ/kg	$\hat{s}$ kJ/kg K
sat	0.88573	2529.5	2706.6	7.1271
150	0.95964	2576.9	2768.8	7.2795
200	1.08034	2654.4	2870.5	7.5066
250	1.19880	2731.2	2971.0	7.7085
300	1.31616	2808.6	3071.8	7.8926
400	1.54930	2966.7	3276.5	8.2217
500	1.78139	3130.7	3487.0	8.5132
600	2.01297	3301.4	3704.0	8.7769
700	2.24426	3478.8	3927.7	9.0194
800	2.47539	3663.2	4158.3	9.2450
900	2.70643	3854.5	4395.8	9.4565
1000	2.93740	4052.5	4640.0	9.6563
1100	3.16834	4257.0	4890.7	9.8458
1200	3.39927	4467.5	5147.3	10.0262
1300	3.63018	4683.2	5409.3	10.1982

$P = 300$ kPa

T °C	$\hat{v}$ m³/kg	$\hat{u}$ kJ/kg	$\hat{h}$ kJ/kg	$\hat{s}$ kJ/kg K
sat	0.60582	2543.6	2725.3	6.9918
150	0.63388	2570.8	2761.0	7.0778
200	0.71629	2650.7	2865.5	7.3115
250	0.79636	2728.7	2967.6	7.5165
300	0.87529	2806.7	3069.3	7.7022
400	1.03151	2965.5	3275.0	8.0329
500	1.18669	3130.0	3486.0	8.3250
600	1.34136	3300.8	3703.2	8.5892
700	1.49573	3478.4	3927.1	8.8319
800	1.64994	3662.9	4157.8	9.0575
900	1.80406	3854.2	4395.4	9.2691
1000	1.95812	4052.3	4639.7	9.4689
1100	2.11214	4256.8	4890.4	9.6585
1200	2.26614	4467.2	5147.1	9.8389
1300	2.42013	4683.0	5409.0	10.0109

$P = 400$ kPa

T °C	$\hat{v}$ m³/kg	$\hat{u}$ kJ/kg	$\hat{h}$ kJ/kg	$\hat{s}$ kJ/kg K
sat	0.46246	2553.6	2738.5	6.8958
150	0.47084	2564.5	2752.8	6.9299
200	0.53422	2646.8	2860.5	7.1706
250	0.59512	2726.1	2964.2	7.3788
300	0.65484	2804.8	3066.7	7.5661
400	0.77262	2964.4	3273.4	7.8984
500	0.88934	3129.2	3484.9	8.1912
600	1.00555	3300.2	3702.4	8.4557
700	1.12147	3477.9	3926.5	8.6987
800	1.23722	3662.5	4157.4	8.9244
900	1.35288	3853.9	4395.1	9.1361
1000	1.46847	4052.0	4639.4	9.3360
1100	1.58404	4256.5	4890.1	9.5255
1200	1.69958	4467.0	5146.8	9.7059
1300	1.81511	4682.8	5408.8	9.8780

Appendix B: Introductory Letter

Appendix C: Plagiarism Test Results